10

Probabilistic approaches for the prediction of forest fire danger using optical and thermal satellite data

Carmine Maffei[a], *Roderik Lindenbergh*[b], *and Massimo Menenti*[b,c]

[a]**Consorzio MedITech – Mediterranean Competence Centre 4 Innovation, Naples, Italy**

[b]**Department of Geoscience & Remote Sensing, Delft University of Technology, Delft, Netherlands**

[c]**State Key Laboratory of Remote Sensing Science, Chinese Academy of Sciences, Aerospace Information Research Institute, Lanzhou, China**

KEY CONCEPTS

- Observations of vegetation condition are covariates of fire burned area, duration, and rate of spread.
- Land surface temperature anomaly and the perpendicular moisture index are independent observations of live fuel condition.
- We achieved comparable or better performance than the Fire Weather Index in predicting probability of extreme fire events.
- A physical interpretation of results is proposed.

Satellite Remote Sensing for Forest and Environmental Monitoring
https://doi.org/10.1016/B978-0-443-40296-8.00010-0

1 Introduction

Forest fires are a major driver of ecosystem disturbance at a global scale (Bond et al., 2005; Krebs et al., 2010; Pyne et al., 1996). They affect the biogeochemical cycle (Thonicke et al., 2008), are a source of atmospheric emissions (Lehsten et al., 2009; Parker et al., 2016; van der Werf et al., 2010), alter the net carbon balance (Lasslop et al., 2019; Seidl et al., 2014), disturb forest structure (Harvey et al., 2016), and cause long-term changes in soil properties (Certini, 2005; Bowd et al., 2019). Fires also condition anthropic activities as they threaten human lives (Viegas, 2009), have a negative effect on quality of life (Reisen et al., 2015; FAO, 2007), and cause substantial economic loss (Montagné-Huck and Brunette, 2018; Pellegrini et al., 2018).

Fires are controlled by multiple static and dynamic drivers related to topography, land cover, climate, weather, and anthropic activity (Littell et al., 2016; Lasslop and Kloster, 2017; Mhawej et al., 2015). Among these, weather is an active driver of live and dead fuel moisture (Ustin et al., 2009; Trenberth et al., 2014; Williams and Abatzoglou, 2016). Fuel moisture has in turn a direct effect on fire occurrence and behaviour, as the proportion of water in live and dead fuels controls ignition delay, probability of extinction, and rate of spread (Chuvieco et al., 2009; Rothermel, 1972; Finney et al., 2013; Wilson, 1985). The role of fuel moisture is thus crucial in predicting fire characteristics (Ustin et al., 2009; Rossa and Fernandes, 2017; Rossa et al., 2016), as it controls the probability distribution of burned area and rate of spread (Podschwit et al., 2018; Flannigan et al., 2016). As a result, in areas experiencing prolonged droughts and heat waves, such as the Mediterranean basin, altered meteorological patterns create the preconditions for increased frequency and intensity of forest fires (Gudmundsson et al., 2014; Lindner et al., 2010).

Society is faced with the need to manage forest fires with preparedness and response efforts aimed at increasing the security of citizens and properties, and at preserving the services and the natural development of the biomes being affected. Such efforts encompass mitigation, preparedness, response, and recovery (Mohamed Shaluf, 2008; Gunes and Kovel, 2000; Oliveira et al., 2017). Concerning preparedness, forest managers and civil protection agencies work with concepts like fire hazard, danger, and risk. Hazard refers to fuel available for burning, i.e., fuel type, amount, and condition. Risk is a measure of the probability of a fire to ignite and spread. Danger is a measure of the difficulty to control fires and thus refers to fire occurrence and behaviour (FAO, 1986). Personal conversations with managers of *Carabinieri* (Italian national gendarmerie) Forest Fire Protection Information Unit (*Nucleo Informativo Antincendio Boschivo*, NIAB), the Italian Civil Protection Department (*Dipartimento della Protezione Civile*),

and the *Entente Valabre* (the coordinating organization of several South France and Corsica departments and departmental fire services) highlighted a clear need for improved prediction of fire occurrence and fire behaviour as an essential element of fire prevention services, or more specifically, the prediction of emergency conditions (Mazzetti et al., 2009).

Several fire danger rating systems have been developed worldwide to support fire prevention (Allgöwer et al., 2003). These are typically based on the evaluation of biophysical and environmental variables that control fire occurrence and behaviour, and on the provision of one or more time-dependent indices in the form of maps. The National Fire Danger Rating System used in the United States is a collection of fuel condition and fire behaviour indicators computed from meteorological measurements, fuel models, climate class, and slope (Burgan, 1988; Deeming et al., 1977). Fuel condition components are a collection of descriptors of the water content of two classes of live fuels and four classes of dead fuels. The McArthur Forest Fire Danger Index used in Australia works along similar principles, but only contains one drought index related to dead fuels moisture (Griffiths, 1999; McArthur, 1967; Keetch and Byram, 1968). The Fire Weather Index (FWI) system is based on the progressive processing of meteorological measurements for the production of three dead fuels moisture codes and three fire behaviour indices, and does not include any model of live fuels moisture (Van Wagner, 1987). The FWI system has been effectively used to map fire danger in several areas worldwide, including Europe (San-Miguel-Ayanz et al., 2012; de Groot and Flannigan, 2014).

A common trait of fire danger indices is their dependence on meteorological input. This is because both fire occurrence and behaviour are controlled by live and dead fuel moisture content, which in turn are determined by the interaction of vegetation, litter, and dead woody material in the topsoil with weather and topography (Rothermel, 1972, 1991; Van Wagner, 1987; Andrews, 2007; Yebra et al., 2013; Finney, 1998). Indeed, fire danger rating systems model fuel moisture content from meteorological measurements and then use computed values to produce one or more indices that serve as predictors of fire occurrence and behaviour. However, the use of modelled rather than measured fuel moisture content results in a certain degree of approximation due to the simplifying assumptions this implies, especially with respect to live fuels (Ruffault et al., 2018; Schunk et al., 2017). In fact, the link between live fuel moisture content (LFMC) and weather forcing is dependent on the structural and physiological characteristics of plants, which are species-specific (Jolly and Johnson, 2018; Pellizzaro et al., 2007b). Nevertheless, LFMC is essential in predicting fire behaviour (Jolly, 2007; Rossa and Fernandes, 2017). From a source data perspective, most fire danger rating services are either based on values from point weather measurements—e.g., automated weather stations, and computed indices are only valid in a limited area around the

point of data collection (Schlobohm and Brain, 2002; Walding et al., 2018; Chowdhury and Hassan, 2015a)—or from coarse resolution-weather forecasts from meteorological services, which lead to maps at a scale that might not be suitable for fire management purposes at local level (San-Miguel-Ayanz et al., 2012; Martell, 2007; North et al., 2015).

Direct observation of LFMC is desirable to enable better predictions of fire occurrence and evaluation of fire danger indices (Ruffault et al., 2018; Jolly, 2007; Rossa and Fernandes, 2017; Ustin et al., 2009). This outlines a clear opportunity for Earth Observation technologies, as they provide repeated and frequent observations of land surface conditions (Allgöwer et al., 2003; Ma et al., 2019; Yebra et al., 2013). Most approaches for the use of remote sensing data in fire danger mapping focussed on relating land surface temperature (LST), spectral indices of vegetation moisture content, radar backscatter, or indirect measures of plant stress to danger indices and fire occurrence. Time series of the Normalized Difference Water Index (Gao, 1996) were found to be related to the seasonality of fire occurrence (Huesca et al., 2014, 2009). The Normalized Difference Water Index was also used in conjunction with satellite estimates of LST to predict fire danger (Abdollahi et al., 2018). The Global Vegetation Moisture Index (Ceccato et al., 2002) was used in combination with LST and a few landscape factors to predict fire occurrence (Pan et al., 2016). Radar backscatter was related to vegetation moisture and fire danger (Hunt et al., 2011; Leblon et al., 2002; Abbott et al., 2007), although it is acknowledged that it is also affected by many other surface properties (Leblon et al., 2016).

With regards to the prediction of emergency conditions, any assessment of remote sensing observables of vegetation status should be translated into an estimation of the probability of either exceptional fire occurrence—this meaning the number of fires occurring in an area in a period of time exceeding a given threshold—or extreme fire events, i.e., whose characteristics exceed a given value (Podschwit et al., 2018; Flannigan et al., 2016; Syphard et al., 2018; Finney, 2005). In fact, several studies showed how optical and thermal remote sensing of forests can be used to predict fire occurrence (Abdollahi et al., 2018; Dasgupta et al., 2006). Other studies have shown that time series of optical vegetation spectral indices and of LST, as proxies of plant water stress, are related to fire occurrence (Maselli et al., 2003; Slingsby et al., 2020). LST was also used to model energy budgets (Vidal et al., 1994; Nolan et al., 2016) and to estimate enthalpy at preignition (Dasgupta et al., 2006) and predict fire occurrence. Fire occurrence was also related to LST anomaly (Manzo-Delgado et al., 2004; Matin et al., 2017; Pan et al., 2016), although there is no shared definition of this parameter.

However, fire danger also refers to fire behaviour (Ruffault et al., 2018). Indeed, fire danger models are meant not only to predict fire occurrence, but also to provide a measure of expected fire behaviour. In this sense,

any attempt to respond to the identified need to improve fire danger models (Ruffault et al., 2018) would require an understanding of remote sensing potential in predicting fire characteristics either deterministically (Dasgupta et al., 2007) or probabilistically (Flannigan et al., 2016). The latter would be more suited to fulfil the need of fire managers, as their interest is in the prediction of the probability of extreme events (Podschwit et al., 2018; Flannigan et al., 2016; Syphard et al., 2018; Finney, 2005). To the best of the authors' knowledge, no research prior to the case study hereby reported has been published that uses remote sensing measurements to predict fire behaviour characteristics. In broader terms, it was not yet known to what extent remote sensing of prefire forest conditions could be used to predict fire behaviour characteristics and to assess the probability of extreme events.

Supporting this approach, the authors found that the probability distribution functions of burned area and fire duration are related to prefire satellite observations of LST anomaly (Maffei et al., 2018), and that probability distribution functions of burned area and rate of spread are related to prefire satellite observations of the Perpendicular Moisture Index (PMI) (Maffei and Menenti, 2014, 2019). These initial results have the potential to enable the prediction of the probability of an extreme event, conditional to ignition, as a function of remote sensing measurements.

In the following sections, it will be further explored whether LST anomaly is related to the probability distribution function of rate of spread; how LST anomaly and PMI compare to each other and against traditional fire danger tools such as the FWI system in predicting forest fire characteristics; whether LST anomaly and PMI can be considered independent; and how they can be jointly used to improve the prefire prediction of the probability of extreme events. To this end, LST anomalies were processed from daily MODIS LST datasets and PMI maps were produced from MODIS surface reflectance 8-day composites. Fire data were then intersected with PMI, LST anomaly, and FWI components maps. Fire burned area, duration and rate of spread were then analysed to identify the best-fitting parametric model describing their respective probability distribution. This allowed the computation of probability distributions of fire characteristics conditional to LST anomaly, PMI, and FWI system components. Trend analysis and likelihood ratio tests were then used to evaluate the performance of LST anomaly, PMI, and FWI system components as covariates of burned area, fire duration, and rate of spread. Finally, a model was developed jointly using LST anomaly and PMI to predict those fire characteristics for which both proved to be a strong covariate (Fig. 10.1). It is hereby acknowledged that material in this case study is widely based on published results (Maffei et al., 2021).

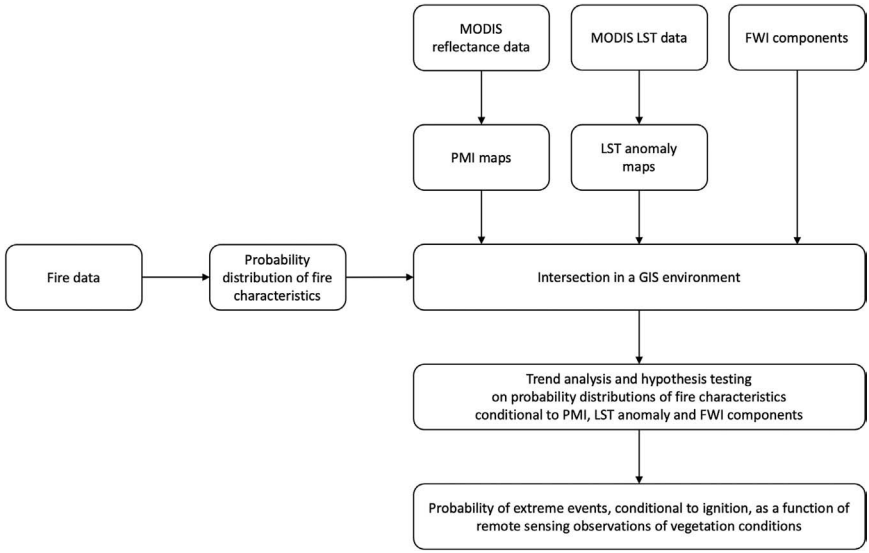

FIG. 10.1 Flow chart describing the logic of this study.

2 Materials and methods

2.1 Study area

Campania, Italy (40.83°N, 14.13°E, 13,595 km^2, Fig. 10.2), is one of the most densely populated and fire-affected regions in Mediterranean Europe (Modugno et al., 2016; San-Miguel-Ayanz et al., 2018). Landscape is divided into two main geomorphological areas. Western Campania alternates rocky coasts and alluvial plains. The climate is typically Mediterranean, with average yearly rainfall between 800 and 1000 mm. Summers are hot and dry, while the maximum rainfall is recorded in winter. The eastern part of the region comprises mountains and hills. Temperature patterns are determined by altitude, while yearly rainfall reaches 1500 mm, with a maximum in autumn and a minimum in summer (Amato and Valletta, 2017; Ducci and Tranfaglia, 2008; Fratianni and Acquaotta, 2017). Agricultural lands (56% of the region), forests, and seminatural areas (38%) dominate the land cover. Among agricultural lands, arable fields are prevalent, followed by fruit trees, olive groves, and vineyards. Among forest and seminatural areas, broad-leaved forests largely dominate.

2.2 Data

2.2.1 Fire data

For this study, the Forest Fire Protection Information Unit of Carabinieri (Italian national gendarmerie) provided a database of fires recorded

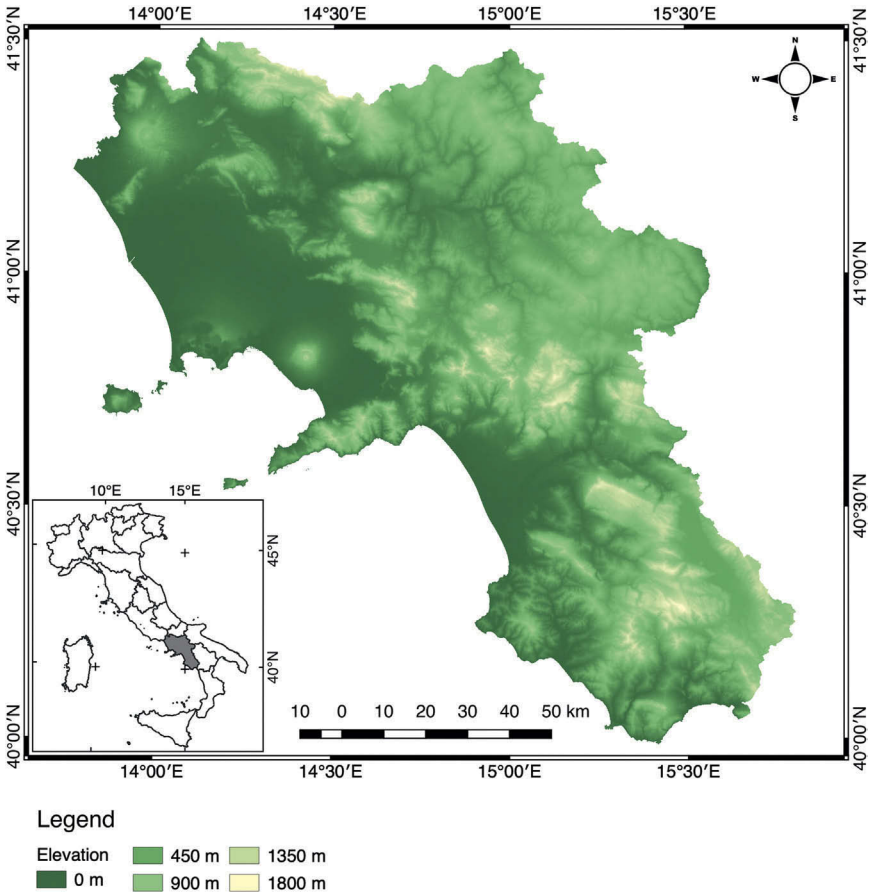

FIG. 10.2 Study area. Elevation map of Campania, the study area of this research. Landscape is divided along the longitudinal gradient in two main geomorphologically and climaticlly different areas. *From Maffei, C., 2022. Remote sensing-based prediction of forest fire characteristics. https://doi.org/10.4233/uuid:8938bc7b-27e7-4b72-b744-1d8a1b0928a5.*

in Campania between 2003 and 2011. This law enforcement agency is in charge, among other responsibilities, of burned area inventorying. The dataset details for each event: cartographic coordinates of the centroid of burned area, date, and time of initial spread and fire extinction, final burned area, and presumed causes. While the Carabinieri record the burnt scar perimeters on a fire-by-fire basis, according to conventional practices of field surveying with GPS receivers and desk digital cartography, these were not provided for this study.

Apart from burned area, additional fire behaviour attributes that can be retrieved from the dataset are fire duration and rate of spread. Fire duration is evaluated as the difference, in hours, between fire inception

and extinction. The rate of spread is calculated from the burned area and fire duration in the simplified assumption of a circular fire growing at a constant rate, in every direction, throughout its duration on a flat and uniform surface.

On average, 838 fires were recorded every year. The mean burned area was 6.5 ha, the mean fire duration was 9.6 h, and the mean rate of spread was 22.1 m/h. 99.7% of fires had an anthropic cause: 73.9% were due to arson, 10.0% to unintentional anthropic activity, while 15.8% were reported as unclassified anthropic (either arson or unintentional). A distinct fire season can be observed in the summer, as 82% of fires and 89% of burned area are recorded between June and September. Subsequently, a subset of 4949 events was extracted from the database for further analysis, consisting of all fires that occurred in natural areas only from June, July, August and September 2003–2011.

2.2.2 MODIS land surface temperature and reflectance data

Remote sensing datasets used in this research were the Aqua-MODIS Level 3 collection 6 LST (MYD11A1) and surface reflectance (MYD09A1) products. Level 3 products are standardized science-ready geophysical variables mapped on a fixed global grid (Masuoka et al., 1998). MYD11A1 contains daily gridded diurnal and nocturnal LST estimates at a conventional resolution of 1 km, along with quality assurance (QA) metadata. A complete time series of MYD11A1 granules covering the years from 2003 to 2017 was used in this research, only retaining pixel data marked as clear-sky and good quality (Xu and Shen, 2013; Van Nguyen et al., 2015; Maffei et al., 2018). MYD09A1 is a product containing 8-day composited reflectance at 500-m resolution (Vermote et al., 1997). Tiles from June, July, August and September for the years 2003–2011 were retrieved and, likewise LST, masked against QA, to ensure only good quality reflectance estimates were retained (Vermote et al., 2015; Maffei and Menenti, 2019).

2.2.3 Fire weather index

The FWI system is based on the processing of daily readings of temperature, relative humidity, wind speed, and precipitation for the production of six fire danger indicators (Van Wagner, 1987). The Fine Fuel Moisture Code (FFMC), the Duff Moisture Code (DMC) and the Drought Code (DC) model the moisture content of dead forest fuels. The Initial Spread Index (ISI) is calculated from FFMC and wind speed. ISI is generally related to the burned area. The Build-Up Index (BUI) is computed from DMC and DC to represent fuel consumption. The FWI is a comprehensive indicator calculated by combining ISI and BUI to synthesize all the fire danger indicators of the FWI system. FWI forecasts are related to the energy output rate of a fire. Daily layers of the FWI system components

used in this study are those from NASA's Global Fire Weather Database (Field et al., 2015; Molod et al., 2015), available at a resolution of 0.25° × 0.25°.

2.3 Approach

2.3.1 *Retrieval of land surface temperature anomaly*

In this study, LST anomaly was evaluated against a reference climatology constructed from the time series of daily diurnal Aqua-MODIS LST (Alfieri et al., 2013) by means of the harmonic analysis of time series (HANTS) algorithm (Menenti et al., 1993, 2016). HANTS handles the Fourier analysis as a least squares curve fitting problem within an iterative approach. Series comprising the first three harmonics were fit to the data with two different methods:

1. HANTS was executed on yearly sequences 2003–2011 of daily LST data individually to construct annual models of daily LST (Xu and Shen, 2013). The objective of this approach was the removal of LST variability due to undetected cloud contamination and varying observation geometry while modelling LST annual variation. The result was a collection of new annual series of daily LST maps, one for each year being considered, computed from the identified harmonic components. These were used as representative of actual measurements.
2. The algorithm was executed on the whole 2003–2017 data set, with a base period of one year, to construct a pixel-wise daily climatology of LST (Alfieri et al., 2013). The output of this process is a new series of daily LST maps computed from the identified harmonic components, representative of daily climatological values of LST (Maffei et al., 2018).

Daily LST anomaly was then evaluated as the LST value in the annual models minus the value in the climatology.

Fig. 10.3 depicts one year of clear-sky Aqua-MODIS LST retrievals in a sample pixel within the study area, along with the corresponding LST annual model and the LST climatology. The annual model captures LST variation throughout the year, while filtering its variability. LST climatology shows a distinct pattern. In this example, the annual model of clear-sky LST is higher than the clear-sky LST climatology for most of the year, meaning that a positive LST anomaly was recorded.

2.3.2 *Perpendicular moisture index (PMI)*

LFMC is the percentage mass of water in leaf tissues over dry leaf mass. This key variable in fire danger assessment directly controls flame

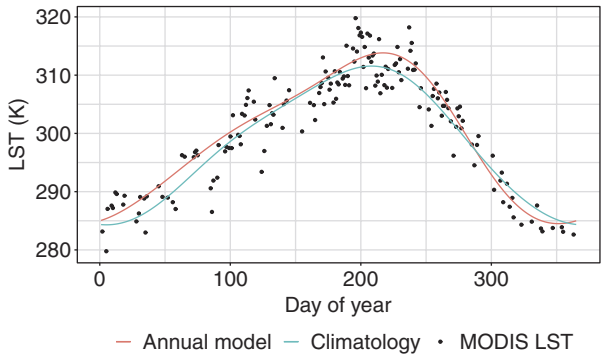

FIG. 10.3 HANTS modelling of LST. Aqua-MODIS LST data, LST annual model and LST climatology observed in year 2007 at position 40°50′40″N, 14°8′56″E. *From Maffei, C., 2022. Remote sensing-based prediction of forest fire characteristics. https://doi.org/10.4233/uuid:8938bc7b-27e7-4b72-b744-1d8a1b0928a5.*

propagation (Carlson and Burgan, 2003; Hunt et al., 2013; Rothermel, 1972, 1991; Van Wagner, 1977; Finney, 1998; Andrews, 2007). The remote sensing proxy for LFMC used in this study is PMI (Maffei and Menenti, 2014), a spectral index specifically designed to maximize its sensitivity to LFMC variability. It was developed from the observation that, in the plane defined by MODIS reflectance at 0.86 μm (band 2) and 1.24 μm (band 5), the isolines of LFMC are straight and parallel. The PMI is thus evaluated as the distance of reflectance points from a reference line:

$$\mathrm{PMI} = -0.73 \times \left(R_{1.24\mu m} - 0.94 \times R_{0.86\mu m} - 0.028\right). \tag{10.1}$$

In this sense, PMI is a direct measure of LFMC, with higher values corresponding to higher moisture content.

2.3.3 *Parametric distributions of fire characteristics*

To evaluate the distribution of fire behaviour characteristics conditional to LST anomaly, PMI, and FWI system components, parametric distributions describing burned area, fire duration, and rate of spread in the study area were first identified. Tested distributions were selected from existing literature (Weber and Stocks, 1998; Corral et al., 2008; Haydon et al., 2000; Baker, 1989; Cumming, 2001; Moritz, 1997; Reed and McKelvey, 2002), and included normal, log-normal, exponential, gamma, generalized extreme value (GEV) and Weibull. The range of reported distributions highlights that no single model can be identified to describe burned area and fire duration distribution globally, due to the diversity of encompassed terrain, climate, ecology, and forest fire management practices (Cui and Perera, 2008; Reed and McKelvey, 2002), and that the closest fitting model needs to be identified on a regional basis.

Available fire data were first scaled and log-transformed, so to have positive values only. Log-transformed data were then fitted to the named distribution through the minimization of the Anderson-Darling distance (Anderson and Darling, 1954):

$$\mathrm{AD} = n\int_{-\infty}^{+\infty} \frac{[F_n(x) - F(x)]^2}{F(x)\times[1-F(x)]} dF(x), \tag{10.2}$$

Where $F(x)$ is the model cumulative distribution function and $F_n(x)$ is the empirical cumulative distribution of the sample. The closest fitting model for each fire characteristic was retained as a basis for further analyses (Hernandez et al., 2015; Maffei et al., 2018).

2.3.4 Conditional distributions of fire characteristics

Prior to further analyses, fires in the dataset were intersected with maps of LST anomaly, PMI, and FWI system components in a GIS environment. Thus each event was associated with the corresponding LST anomaly value recorded in the day previous to the event, the PMI value recorded in the previous 8-day compositing period, and the values of the FWI system components recorded on the day of the event (Maffei et al., 2018, 2021; Maffei and Menenti, 2019). Observations of PMI, LST anomaly, and FWI system components associated with fires were grouped in their respective ten decile bins. The parameters of best-fitting distributions for log-transformed burned area, log-transformed fire duration, and log-transformed rate of spread were assessed in each bin through the minimization of the Anderson-Darling statistic. The corresponding 95% confidence intervals were then evaluated by means of 1000 bootstrap estimations.

Trends in the values of the parameters of the probability distributions with respect to LST anomaly, PMI, and the FWI system components were assessed and compared by means of linear regressions (coefficient of determination and p-value), Sen's slope magnitude (Sen, 1968), and Mann–Kendall test (Kendall, 1975; Mann, 1945). A likelihood ratio test was adopted to evaluate the probability distribution functions conditional to LST anomaly, PMI, and the FWI system components (alternative models) against the corresponding unconditional models fitting all data (null models). Significance was set at 0.05 for linear regressions, the Mann–Kendall test, and the likelihood ratio test.

2.3.5 Probability of extreme events conditional to ignition

An extreme event is hereby defined as a fire whose characteristic is larger than the 95th percentile of the values recoded in the database. The evaluation of the probability of extreme events conditional to ignition as a function of LST anomaly (alternatively PMI) builds on the conditional

probability distribution functions identified in the previous section. The dependence of distribution parameters on LST anomaly (alternatively PMI) was modelled by means of linear regressions.

A similar approach was adopted to model the probability of extreme events as a function of both LST anomaly and PMI. The bidimensional space spanned by LST anomaly and PMI was partitioned into 100 bins determined by the previously defined decile intervals. The parameters of the probability distribution functions were evaluated in each bidimensional bin through the minimization of the Anderson-Darling statistic. Their dependence on LST anomaly and PMI was then modelled by means of a multiple linear regression. The performance of the derived linear models was then assessed by using the leave-one-out cross-validation (LOOCV).

3 Experimental results

3.1 Probability models of fire characteristics

Log-transformed burned area, fire duration, and rate of spread were fitted to normal, log-normal, exponential, gamma, GEV and Weibull distributions, and the corresponding Anderson-Darling statistics are reported in Table 10.1. Normal is the closest fitting distribution of log-transformed burned area, while GEV is the closest model for log-transformed fire duration and Weibull for log-transformed rate of spread. The corresponding Q–Q plots are reported in Fig. 10.4.

TABLE 10.1 Anderson-Darling statistic values for tested distributions. Lower values indicate a closer fit.

Model	Log-transformed burned area	Log-transformed fire duration	Log-transformed rate of spread
Normal	7.2	52.3	20.3
Log-normal	16.7	20.4	40.8
Exponential	1347	1387	1559
Gamma	11.0	28.7	33.1
Generalized extreme value (GEV)	10.5	10.5	39.6
Weibull	25.2	134	8.2

From Maffei, C., Menenti, M., 2019. Predicting forest fires burned area and rate of spread from pre-fire multispectral satellite measurements. ISPRS J. Photogramm. Remote Sens. 158, 263–278. https://doi.org/10.1016/j.isprsjprs.2019.10.013.

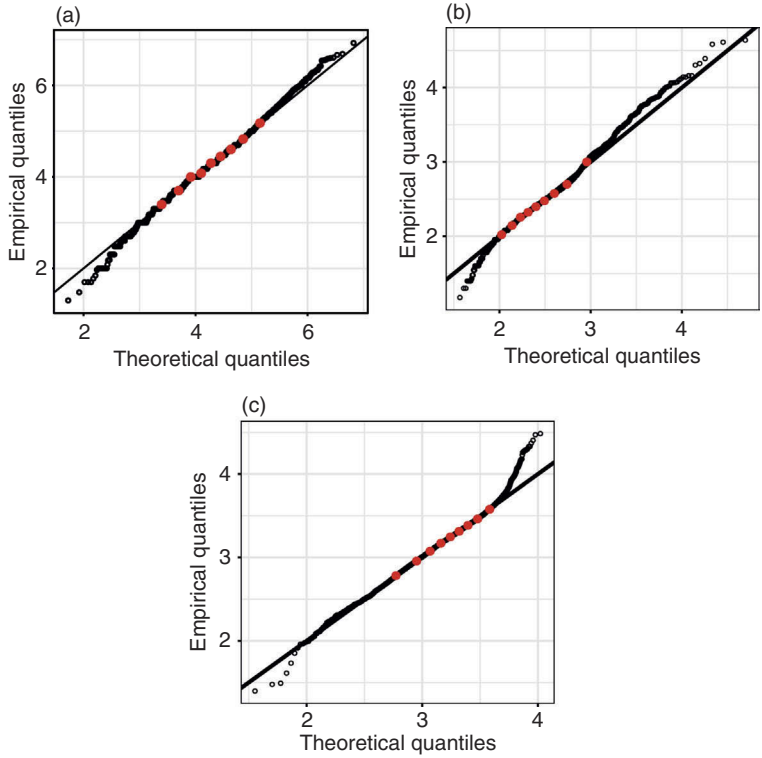

FIG. 10.4 Q–Q plots. Q–Q plots of the normal distribution of log-transformed burned area (a), of the GEV distribution of log-transformed fire duration (b) and of the Weibull distribution of log-transformed rate of spread (c). Red circles indicate the deciles of the distributions. *From Maffei, C., 2022. Remote sensing-based prediction of forest fire characteristics. https://doi.org/10.4233/uuid:8938bc7b-27e7-4b72-b744-1d8a1b0928a5.*

3.2 Comparing LST anomaly and PMI performance in predicting fire characteristics

The scatterplot of LST anomaly and PMI values associated with fire events shows that these two remote sensing observations are substantially unrelated (Fig. 10.5). This is reflected in the dispersion of burned area, fire duration, and the rate of spread in decile bins of LST anomaly and PMI (Fig. 10.6). Burned area appears to be dispersed towards higher values with increasing LST anomaly and decreasing PMI (lower LFMC). Dispersion of fire duration is towards higher values with increasing LST anomaly, whereas no trend is observed against PMI. Conversely, the rate of spread appears to be dispersed towards lower values with increasing PMI (higher LFMC), while only a weak decreasing trend can be noted against LST anomaly.

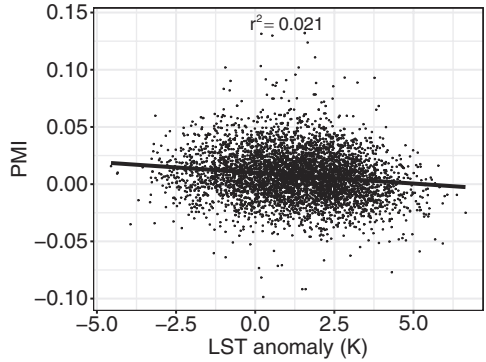

FIG. 10.5 PMI versus LST. Scatterplot of PMI versus LST anomaly values associated with fire events. *From Maffei, C., Lindenbergh, R., Menenti, M., 2021. Combining multi-spectral and thermal remote sensing to predict forest fire characteristics. ISPRS J. Photogramm. Remote Sens. 181, 400–412. https://doi.org/10.1016/j.isprsjprs.2021.09.016.*

The analysis of the probability distribution functions of burned area, fire duration and rate of spread in decile bins of LST anomaly and PMI (conditional distributions) further demonstrated that these two satellite observables are differently related to fire characteristics. The mean of the normal distribution of log-transformed burned area varies with both LST anomaly (r^2 = 0.81, $p < 0.001$) and PMI (r^2 = 0.80, $p < 0.001$), showing comparable Sen's slope magnitude (Fig. 10.7, Table 10.2). Standard deviation follows a significant trend only against LST anomaly (r^2 = 0.52, $p < 0.05$), whereas a constant value fits most confidence intervals of this parameter in decile bins of PMI. The latter is confirmed by trend analysis, as Mann–Kendall test fails to reject the null hypothesis.

Location, scale, and shape of the GEV distribution of log-transformed fire duration conditional to LST anomaly follow strong and significant increasing trends (r^2 = 0.78, 0.79, and 0.87 respectively, $p < 0.001$) with increasing LST anomaly (Fig. 10.8, Table 10.3). The parameter of the GEV distribution of log-transformed fire duration conditional to PMI showing a trend is scale (r^2 = 0.55, $p < 0.05$). However, a constant value of scale would fit most confidence intervals, and indeed Mann–Kendall test fails to reject the null hypothesis for all three GEV parameters conditional to PMI, confirming the absence of a trend with significance 0.05.

Distribution of log-transformed rate of spread conditional to LST anomaly and PMI shows the opposite behaviour as compared to fire duration (Fig. 10.9, Table 10.4). The scale and shape parameters of the Weibull distribution conditional to LST anomaly only show a weak decreasing trend (r^2 = 0.54 and 0.50, respectively), albeit significant ($p < 0.05$). Sen's slope magnitude is low; however, the Mann–Kendall test allows the rejection of the null hypothesis, and the existence of a trend can be accepted

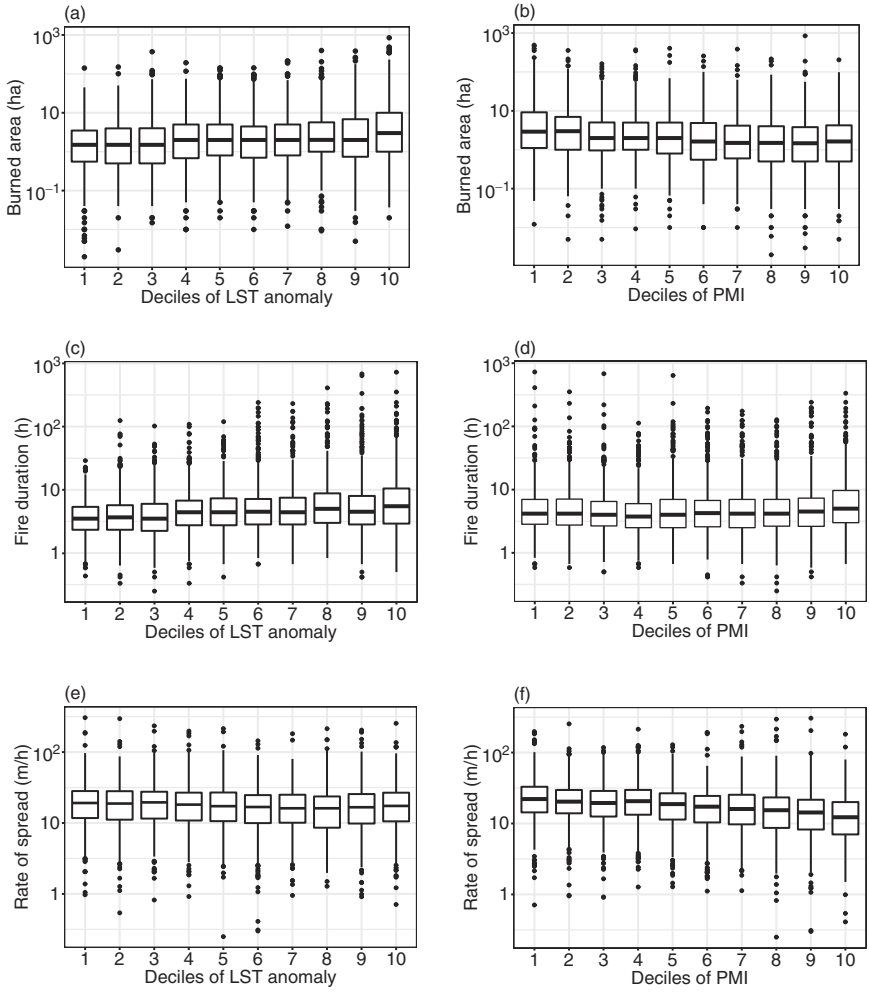

FIG. 10.6 Boxplots of fire characteristics. Boxplots of burned area, fire duration, and rate of spread in decile bins of LST anomaly and PMI. *From Maffei, C., Lindenbergh, R., Menenti, M., 2021. Combining multi-spectral and thermal remote sensing to predict forest fire characteristics. ISPRS J. Photogramm. Remote Sens. 181, 400–412. https://doi.org/10.1016/j.isprsjprs.2021.09.016.*

with significance 0.05. Conversely, the scale and shape conditional to PMI show strong and significant decreasing trends (r^2 = 0.97 and 0.82, respectively, $p < 0.001$) with increasing PMI (corresponding to increasing LFMC) and high Sen's slope magnitude.

The probability distribution functions of the three log-transformed fire characteristics conditional to LST anomaly and PMI allow the rejection of the null (unconditional) model in the likelihood ratio test (Table 10.5), confirming that LST anomaly is a covariate of all three fire characteristics.

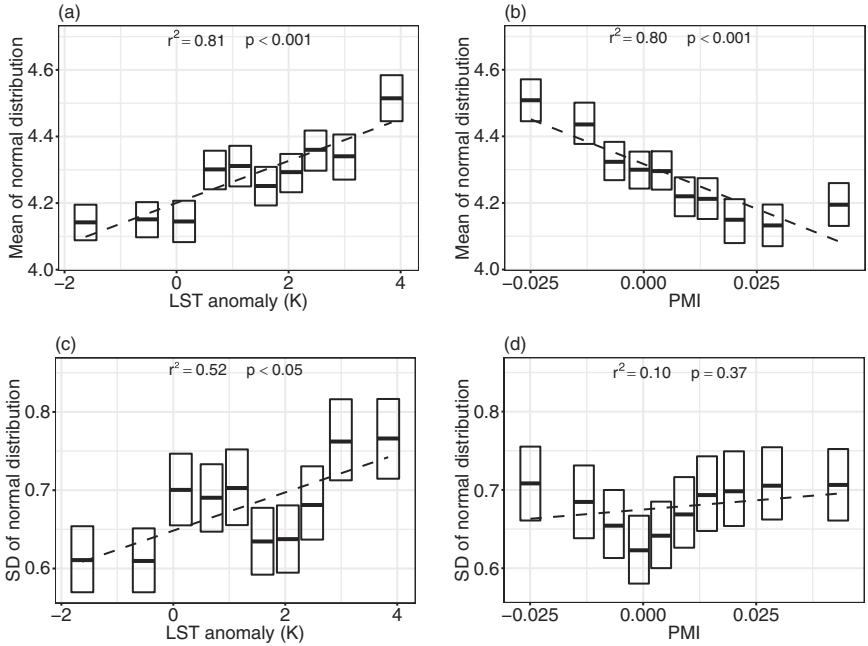

FIG. 10.7 Conditional distributions of burned area. Mean and standard deviation of normal distribution of log-transformed burned area in decile bins of LST anomaly and PMI. *From Maffei, C., Lindenbergh, R., Menenti, M., 2021. Combining multi-spectral and thermal remote sensing to predict forest fire characteristics. ISPRS J. Photogramm. Remote Sens. 181, 400–412. https://doi.org/10.1016/j.isprsjprs.2021.09.016.*

TABLE 10.2 Trend analysis of the parameters of the normal distribution of log-transformed burned area across decile bins of LST anomaly, PMI, and of the FWI system components, reporting coefficient of determination and *p*-value of the linear fit, Sen's slope, and Mann–Kendall test's result.

	Mean				Standard deviation			
	r^2	*p*	Sen's slope	M–K test	r^2	*p*	Sen's slope	M–K test
LST anomaly	0.81	***	0.033	Rejects	0.52	*	0.0124	Rejects
PMI	0.80	***	−0.038	Rejects	0.10	ns	0.0048	Fails
FFMC	0.82	***	0.036	Rejects	0.43	*	0.0050	Fails
DMC	0.89	***	0.028	Rejects	0.78	***	0.0093	Rejects
DC	0.81	***	0.017	Rejects	0.21	ns	0.0095	Fails
ISI	0.92	***	0.036	Rejects	0.21	ns	0.0043	Fails
BUI	0.91	***	0.025	Rejects	0.72	**	0.0075	Fails
FWI	0.96	***	0.034	Rejects	0.31	ns	0.0081	Fails

The *p*-value rating: * Significant at $p \leq 0.05$; ** Highly significant at $p \leq 0.01$; *** Very highly significant at $p \leq 0.001$; ns not significant ($p > 0.05$). Significance level of Mann–Kendall test is 0.05.
From Maffei, C., Lindenbergh, R., Menenti, M., 2021. Combining multi-spectral and thermal remote sensing to predict forest fire characteristics. ISPRS J. Photogramm. Remote Sens., 181, 400–412. https://doi.org/10.1016/j.isprsjprs.2021.09.016.

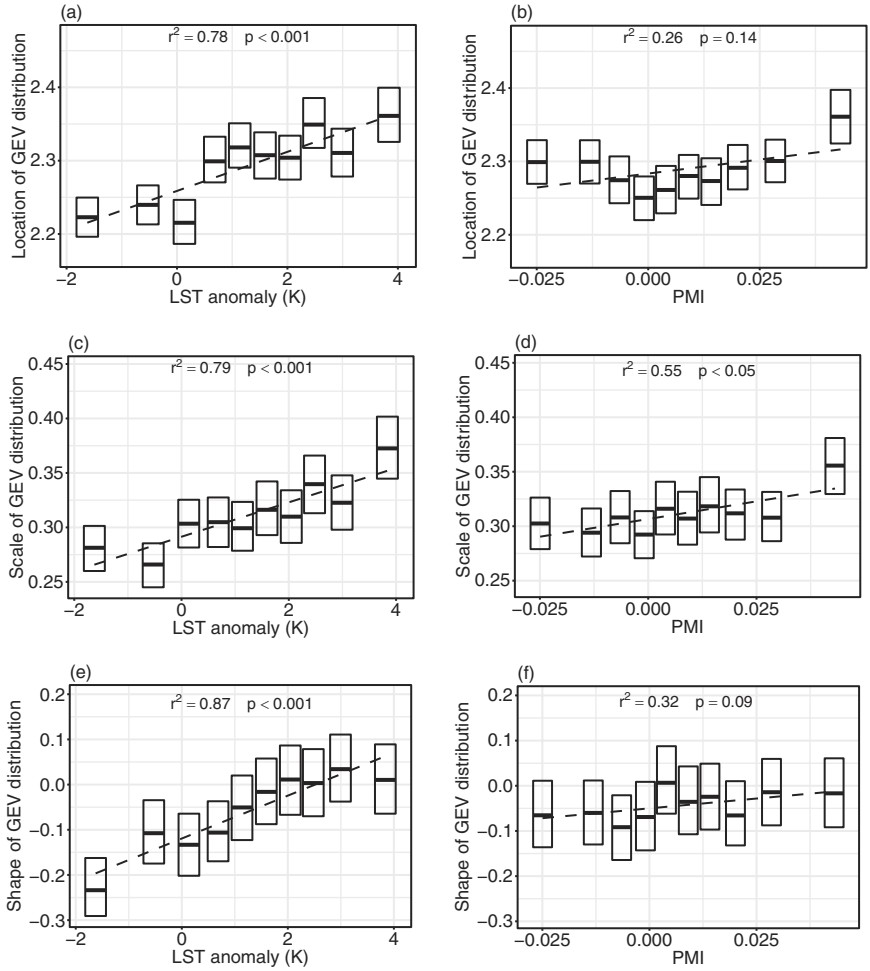

FIG. 10.8 Conditional distributions of fire duration. Location, scale, and shape of the GEV distribution of log-transformed fire duration in decile bins of LST anomaly and PMI. *From Maffei, C., Lindenbergh, R., Menenti, M., 2021. Combining multi-spectral and thermal remote sensing to predict forest fire characteristics. ISPRS J. Photogramm. Remote Sens., 181, 400–412. https://doi.org/10.1016/j.isprsjprs.2021.09.016.*

Similarly, probability models of log-transformed burned area and log-transformed rate of spread conditional to PMI allow the rejection of the unconditional model, whereas the corresponding conditional model of log-transformed fire duration does not. Comparing these findings against trends outlined in Fig. 10.8 and in Table 10.3 leads to the conclusion that PMI is a covariate of burned area and rate of spread, but not of fire duration.

TABLE 10.3 Trend analysis of the parameters of the GEV distribution of log-transformed fire duration across decile bins of LST anomaly, PMI, and of the FWI system components, reporting coefficient of determination and *p*-value of the linear fit, Sen's slope, and Mann–Kendall test's result.

	Location				Scale				Shape			
	r^2	*p*	Sen's slope	M–K test	r^2	*p*	Sen's slope	M–K test	r^2	*p*	Sen's slope	M–K test
LST an.	0.78	***	0.015	Rejects	0.79	***	0.0081	Rejects	0.87	***	0.027	Rejects
PMI	0.26	ns	0.006	Fails	0.55	*	0.0028	Fails	0.32	ns	0.006	Fails
FFMC	0.76	**	0.013	Rejects	0.85	***	0.0083	Rejects	0.70	**	0.012	Rejects
DMC	0.90	***	0.016	Rejects	0.83	***	0.0051	Rejects	0.44	*	0.014	Fails
DC	0.93	***	0.014	Rejects	0.53	*	0.0047	Fails	0.63	**	0.020	Rejects
ISI	0.83	***	0.012	Rejects	0.68	**	0.0086	Rejects	0.41	*	0.012	Fails
BUI	0.95	***	0.016	Rejects	0.80	***	0.0052	Rejects	0.57	*	0.012	Fails
FWI	0.93	***	0.012	Rejects	0.96	***	0.0087	Rejects	0.64	**	0.012	Fails

The *p*-value rating: * Significant at $p \leq 0.05$; ** Highly significant at $p \leq 0.01$; *** Very highly significant at $p \leq 0.001$; ns not significant ($p > 0.05$). Significance level of Mann–Kendall test is 0.05.
From Maffei, C., Lindenbergh, R., Menenti, M., 2021. Combining multi-spectral and thermal remote sensing to predict forest fire characteristics. ISPRS J. Photogramm. Remote Sens. 181, 400–412. https://doi.org/10.1016/j.isprsjprs.2021.09.016.

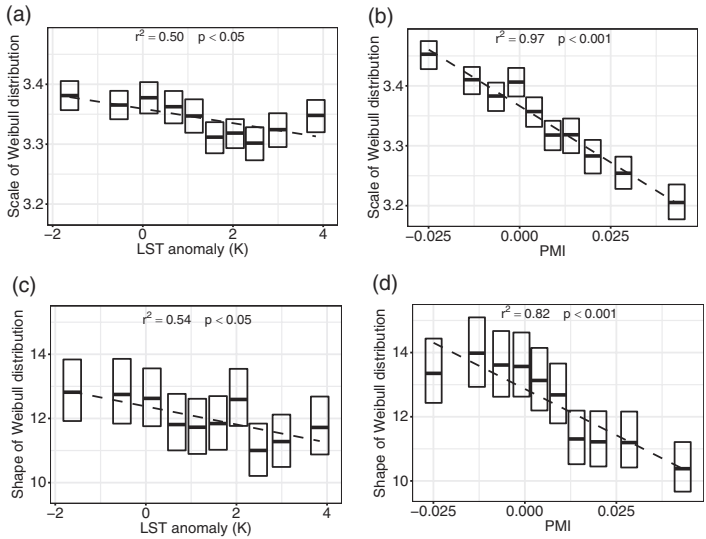

FIG. 10.9 Conditional distributions of rate of spread. Scale and shape of the Weibull distribution of log-transformed rate of spread in decile bins of LST anomaly and PMI. *From Maffei, C., Lindenbergh, R., Menenti, M., 2021. Combining multi-spectral and thermal remote sensing to predict forest fire characteristics. ISPRS J. Photogramm. Remote Sens. 181, 400–412. https://doi.org/10.1016/j.isprsjprs.2021.09.016.*

TABLE 10.4 Trend analysis of the parameters of the Weibull distribution of log-transformed rate of spread across decile bins of LST anomaly, PMI, and of the FWI system components, reporting coefficient of determination and *p*-value of the linear fit, Sen's slope, and Mann–Kendall test's result.

	Scale				Shape			
	r^2	*p*	Sen's slope	M–K test	r^2	*p*	Sen's slope	M–K test
LST anomaly	0.50	*	−0.0077	Rejects	0.54	*	−0.129	Rejects
PMI	0.97	***	−0.0254	Rejects	0.82	***	−0.419	Rejects
FFMC	0.18	ns	−0.0017	Fails	0.03	ns	0.032	Fails
DMC	0.38	ns	−0.0064	Rejects	0.41	*	−0.137	Fails
DC	0.66	**	−0.0098	Rejects	0.57	*	−0.173	Rejects
ISI	0.05	ns	−0.0009	Fails	0.01	ns	0.027	Fails
BUI	0.65	**	−0.0066	Rejects	0.52	*	−0.102	Fails
FWI	0.30	ns	−0.0026	Fails	0.01	ns	−0.025	Fails

The *p*-value rating: * Significant at $p \leq 0.05$; ** Highly significant at $p \leq 0.01$; *** Very highly significant at $p \leq 0.001$; ns not significant ($p > 0.05$). Significance level of Mann–Kendall test is 0.05.
From Maffei, C., Lindenbergh, R., Menenti, M., 2021. Combining multi-spectral and thermal remote sensing to predict forest fire characteristics. ISPRS J. Photogramm. Remote Sens. 181, 400–412. https://doi.org/10.1016/j.isprsjprs.2021.09.016.

TABLE 10.5 Results of the likelihood ratio test. Null model is the one fitting all data. Alternative model is the collection of ten models in decile bins of the candidate covariate. Significance level is 0.05. The alternative models showing the highest likelihood for each fire characteristic are shown in bold.

	Burned area	Duration	Rate of spread
LST anomaly	**Rejects**	**Rejects**	Rejects
PMI	Rejects	Fails	**Rejects**
FFMC	Rejects	Rejects	Fails
DMC	Rejects	Rejects	Fails
DC	Rejects	Rejects	Fails
ISI	Rejects	Rejects	Rejects
BUI	Rejects	Rejects	Rejects
FWI	Rejects	Rejects	Rejects

From Maffei, C., Lindenbergh, R., Menenti, M., 2021. Combining multi-spectral and thermal remote sensing to predict forest fire characteristics. ISPRS J. Photogramm. Remote Sens. 181, 400–412. https://doi.org/10.1016/j.isprsjprs.2021.09.016.

3.3 Assessing the performance of LST anomaly and PMI against the FWI system components

Trend analysis of the parameters of the probability distribution of log-transformed burned area, fire duration, and rate of spread in decile bins of the FWI system components allows a comparison of the performance of prefire remote sensing retrievals of vegetation condition in predicting fire danger against a consolidated fire danger mapping tool based on meteorological data. The mean of the normal distribution of log-transformed burned area shows strong and significant ($p < 0.001$) trends against all FWI system components, with Sen's slope magnitude values mostly comparable with those achieved by LST anomaly and PMI (Table 10.2). Conditional standard deviation is characterized by significant trends against FFMC, DMC, and BUI, but only DMC's Mann–Kendall test allows the rejection of the null hypothesis, i.e., confirms that the alternative hypothesis of the existence of a trend can be accepted. These results are reflected in the likelihood ratio test (Table 10.5), as all alternative models conditional to FWI system components allow the rejection of the unconditional model.

Similar results were found with the parameters of the GEV distribution of log-transformed fire duration (Table 10.3). Location, scale, and shape show significant trends against all FWI system components with strength and Sen's slope magnitude substantially comparable with those against LST anomaly. Further, all the conditional models allow the rejection of the unconditional model (Table 10.5).

The FWI system components do not appear to be good covariates of rate of spread. Scale of the Weibull distribution of log-transformed rate of spread shows significant ($p < 0.01$) trends only against DC and BUI, although with lower strength and Sen's slope magnitude than PMI (Table 10.4). Shape shows significant ($p < 0.05$) trends against DMC, DC, and BUI, but only DC's Mann–Kendall test rejects the null hypothesis of the absence of a trend. For both parameters, this contrasts with the strength and Sen's slope of the trends against PMI. While DC might still be considered a covariate of rate of spread, the corresponding conditional probability model does not allow the rejection of the unconditional model (Table 10.5).

3.4 Predicting the probability of extreme events conditional to ignition

As both LST anomaly and PMI are strong covariates of burned area and are not correlated, it was interesting to compare how the probability of extreme events conditional to ignition varies as a function of LST anomaly and PMI, both individually and jointly. The mean and the stand-

ard deviation of the normal distribution of log-transformed burned area were modelled as linear functions of LST anomaly according to regression lines identified in Fig. 10.7. Similarly, the mean of the normal distribution of log-transformed burned area was modelled as a linear function of PMI, while standard deviation was kept constant. According to the available fire data, the 95th percentile of burned area is 30.0 ha. Plots of the probability of fires larger than 30.0 ha show a marked increase with increasing LST anomaly and decreasing PMI (Fig. 10.10).

A similar approach was used to evaluate the probability of large fires as a joint function of LST anomaly and PMI. The derived linear model fitting the mean of the normal distribution of log-transformed burned area in the 100 bins determined by the decile intervals of LST anomaly and PMI has $r^2 = 0.49$ ($p < 0.001$), whereas the corresponding linear model of the standard deviation has $r^2 = 0.28$ ($p < 0.001$). The leave-one-out cross-validation coefficient of determination is 0.45 and 0.23 for the mean and the standard deviation respectively, showing relative robustness of their linear models as a function of LST anomaly and PMI.

Using as a reference the 2.5%–97.5% percentile range of recorded LST anomaly and PMI values, the probability of large fires conditional to ignition increases from 0.9% to 9.2% with LST anomaly increasing from −2.1 to 4.3 K, and increases from 1.8% to 7.4% with PMI decreasing from 0.052 to −0.032. When the probability of fires exceeding 30.0 ha is modelled as a function of both LST anomaly and PMI, modelled probabilities cover the wider range from 0.5% to 12.7% (Fig. 10.11).

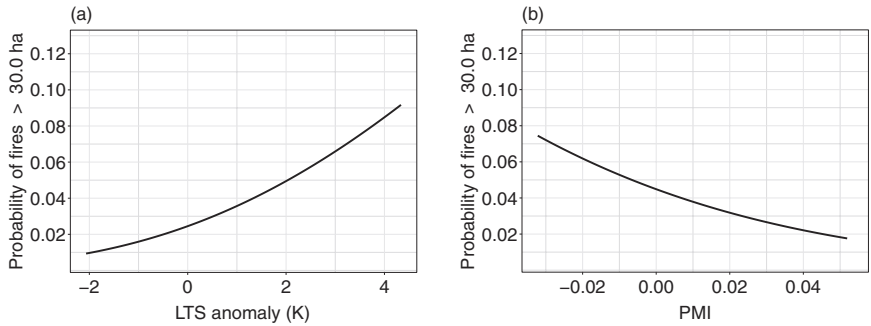

FIG. 10.10 Probability of large fires. Modelled probability of fires larger than 30.0 ha (95th percentile of the values recorded in the study area), conditional to ignition, as a function of LST anomaly and PMI. *From Maffei, C., Lindenbergh, R., Menenti, M., 2021. Combining multispectral and thermal remote sensing to predict forest fire characteristics. ISPRS J. Photogramm. Remote Sens. 181, 400–412. https://doi.org/10.1016/j.isprsjprs.2021.09.016.*

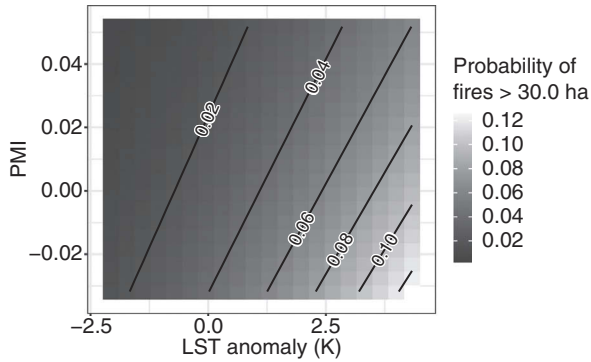

FIG. 10.11 Probability of large fires. Modelled probability of fires larger than 30.0 ha (95th percentile of the values recorded in the study area), conditional to ignition, as a function of both LST anomaly and PMI. Solid lines indicate probability values. *From Maffei, C., Lindenbergh, R., Menenti, M., 2021. Combining multi-spectral and thermal remote sensing to predict forest fire characteristics. ISPRS J. Photogramm. Remote Sens. 181, 400–412. https://doi.org/10.1016/j.isprsjprs.2021.09.016.*

4 Discussion

This case study synthesizes results from previous investigations on multispectral and thermal remote sensing of forest conditions for the prediction of some fire characteristics (Maffei and Menenti, 2019; Maffei et al., 2018, 2021). Its main objective was to evaluate prefire LST anomaly and PMI retrievals as predictors of the probability distribution of burned area, fire duration, and rate of spread conditional to ignition and to assess their performance against the FWI system components. This entailed evaluating and understanding the independence of these two remote sensing observations of live fuel condition to establish an approach for their joint use in the prediction of extreme events. The PMI was designed to be a measure of LFMC (Maffei and Menenti, 2014), and as such it is related to the condition of green vegetation. LST anomaly was initially conceived as a measure of vegetation response to water stress (Alfieri et al., 2013; Maffei et al., 2018), and for this reason it was interpreted with reference to a physiological condition (Leblon, 2005; Chowdhury and Hassan, 2015b; Sobrino et al., 2016; Vidal et al., 1994; Nolan et al., 2016; Dasgupta et al., 2006; Manzo-Delgado et al., 2004; Pan et al., 2016; Matin et al., 2017; Buitrago Acevedo et al., 2017). Indeed, when water stress attains certain levels it triggers plants' transpiration regulation mechanism, and this results in a detectable increase of canopy temperature (Hsiao, 1973; Schulze et al., 1973; Zweifel et al., 2009; Jackson et al., 1981; Nemani and Running, 1989; Kalma et al., 2008; Karnieli et al., 2010; Liu et al., 2016; Buitrago Acevedo et al., 2017).

4.1 Considerations on spatial and temporal granularity of satellite data

Satellite imagery used in this research was at two different resolutions. MODIS optical bands to retrieve the PMI are available at a resolution of 500 m whereas thermal bands, from which LST anomaly is derived, are available at 1000 m. While the operational production of maps of probability of extreme events as a bivariate function of LST anomaly and PMI might require some consideration on the most suitable approach to combine data at different resolutions, from the point of view of the analyses herein this is not relevant. Indeed, each fire was associated with the prefire environmental condition (LST anomaly, alternatively PMI) of the cell in which it was located (1 and 0.25 km^2, respectively), independently of the resolution of the source dataset (Pyne et al., 1996). As will be shortly discussed, these two variables are independent; there is no effect of the differing resolution on the characterization of the prefire environmental conditions of the specific cell containing the fire.

The optical and thermal datasets were different also in terms of temporal structure. LST anomaly was derived from a daily climatology and an annual model of LST, both constructed by means of the HANTS algorithm (Alfieri et al., 2013; Verhoef, 1996; Roerink et al., 2000; Menenti et al., 1993). In this sense, the daily temporal granularity of LST anomaly is inherent in the approach adopted to model it. On the other side, PMI was computed from the 8-day composited MODIS reflectance product. Composited products have the advantage of providing the best cloud-free estimate of the pixel in a standardized grid while compensating for cloud cover and view angle. The coarser temporal granularity was not perceived as an obstacle as during the dry season LFMC only changes abruptly in correspondence with rainfalls (Ruffault et al., 2018) and the use of the prior compositing period in a predictive approach renders temporal sampling less critical. An alternative approach could have been to model PMI variability by means of the HANTS algorithm to gap-fill cloudy pixels and compensate for noise, while retaining a daily coverage, as reported in literature for LST and NDVI (Menenti et al., 1993; Verhoef, 1996; Alfieri et al., 2013; Menenti et al., 2016). However, it is not known whether harmonic analysis is able to capture PMI variability with a reasonable number of harmonics with respect to the available number of observations (Zhou et al., 2016), and investigating this was beyond the objectives of this study.

Analyses reported herein are based on prefire satellite observations of LST anomaly and of PMI. Indeed, each fire was associated with the LST anomaly data from the previous day and to the PMI map of the previous 8-day compositing period. This ensures that results can be adopted in an operational scenario where current observations are used to predict fire characteristics in the following days. This is consistent with the

choice of associating fires with the same day value of the FWI system components. Indeed, FWI maps are available in advance as being produced from forecasts of weather conditions (San-Miguel-Ayanz et al., 2012).

4.2 LST anomaly and PMI as predictors of fire characteristics

LST anomaly appears to capture part of the variability in burned area and fire duration (Fig. 10.6), with increasing values leading to larger fires and longer durations. This is reflected in the parameters of the corresponding conditional probability distribution functions. Both mean and standard deviation of normal distribution of log-transformed burned area conditional to LST anomaly show significant ($p < 0.001$ and $p < 0.05$, respectively) increasing trends (Fig. 10.7) with a high Sen's slope magnitude (Table 10.2). Similarly, location, scale, and shape of the GEV distribution of log-transformed fire duration conditional to LST anomaly are characterized by strong ($r^2 = 0.78$, 0.79, and 0.87) and significant ($p < 0.001$) trends with a high Sen's slope (Table 10.3). These results are further confirmed by the likelihood ratio test, with the conditional (alternative) models allowing the rejection of the unconditional (null) models for both fire characteristics (Table 10.5).

The dispersion of rate of spread in decile bins of the LST anomaly shows a weakly decreasing trend (Fig. 10.6). This is reflected in both scale and shape of the corresponding Weibull distribution. Both parameters exhibit a significant ($p < 0.05$) decreasing trend (Fig. 10.9), albeit less significant and with a much lower Sen's slope magnitude as opposed to PMI (Table 10.4). The Mann–Kendall test confirms that the null hypothesis of absence of trend can be rejected, and the likelihood ratio test further confirms that the alternative model allows the rejection of the null model (Table 10.5). Nevertheless, the weakness of the trend and the relatively low Sen's slope magnitude implies that LST anomaly might not be considered a strong covariate for rate of spread.

Along the same line of reasoning, it can be noted that the dispersion of burned area and rate of spread varies across decile bins of PMI (Fig. 10.6). Increasing values of PMI, corresponding to increasing LFMC, lead to a dispersion of burned area and rate of spread towards lower values. This is further confirmed in the trends of the parameters of the corresponding probability distribution models. The mean of the normal distribution of log-transformed burned area has a strong ($r^2 = 0.80$) and significant ($p < 0.001$) decreasing trend with PMI (Fig. 10.7) with high Sen's slope magnitude (Table 10.2). As opposed to LST anomaly, standard deviation shows no trend, the Mann–Kendall test fails to reject the null hypothesis, and a constant value would be appropriate to describe its variability. The likelihood ratio test confirms that this probability model, which is condi-

tional to PMI, allows the rejection of the unconditional model. Both scale and shape of the Weibull distribution of log-transformed rate of spread show strong (r^2 = 0.97 and 0.82) and significant ($p < 0.001$) trends against PMI (Fig. 10.9), both characterized by a high Sen's slope magnitude (Table 10.4). The likelihood ratio test confirms the rejection of the corresponding null model (Table 10.5).

PMI does not appear to control fire duration. The dispersion of fire duration values does not vary across decile bins of PMI (Fig. 10.6), and the only parameter of the GEV distribution of log-transformed fire duration that shows a significant ($p < 0.05$), yet weak trend is scale (Fig. 10.8). Nevertheless, the Mann–Kendall test fails to reject the null hypothesis, and the absence of a trend cannot be rejected (Table 10.3). Indeed, constant values would fit most confidence intervals across PMI bins (Fig. 10.8) and the likelihood ratio test confirms that the conditional model fails to reject the null model (Table 10.5).

These results are not unexpected. PMI was already demonstrated to be a good predictor of summer fires burned area and rate of spread in the region (Maffei and Menenti, 2019). Results based on LST anomaly were less obvious, as previous analyses focussed on burned area and fire duration only, and the evaluation was performed on events occurring all the year round (Maffei et al., 2018). That said, analyses herein confirm that LST anomaly is a predictor of burned area and fire duration of summer fires. It was also found that LST anomaly is not a strong covariate of rate of spread, albeit the existence of a relationship linking it to the corresponding probability distribution model cannot be ruled out.

4.3 Comparing the predictive performance of LST anomaly and PMI against the FWI system components

Trend analysis and likelihood ratio test were used to compare LST anomaly and PMI versus the FWI system components. This fire danger model was chosen as it proved to be adaptable to various biomes worldwide (de Groot and Flannigan, 2014; Dowdy et al., 2009; San-Miguel-Ayanz et al., 2012; Taylor and Alexander, 2006). LST anomaly and PMI perform as well as FWI in predicting burned area, with the mean of the normal distribution of log-transformed burned area showing strong and significant ($p < 0.001$) trends and comparable Sen's slope magnitude (Table 10.2). While trends in the standard deviation are quite varying and not present in some covariates, all conditional models of log-transformed burned area allow the rejection of the null model (Table 10.5). Similar considerations lead to note that LST anomaly performs similarly to the FWI system components in predicting fire duration (Table 10.3). With

respect to rate of spread, none of the FWI system components show convincing trends of the conditional parameters of the Weibull distribution (Table 10.4). While an exception could be raised for DC, it must be noted that the corresponding conditional model fails to reject the unconditional (null) model (Table 10.5). It can thus be stated that, in the study area, multispectral remote sensing of LFMC (via the PMI) is a good predictor of rate of spread, whereas the FWI system components are not.

4.4 Interpreting results against combustion and propagation processes

LST anomaly and PMI proved to be independent, as noted in Fig. 10.5 and because of their different prediction capability with respect to fire duration and rate of spread. PMI is a spectral index exploiting the different effects of water content on the spectral properties of vegetation in the near infrared and in the shortwave infrared to provide a direct measure of LFMC (Maffei and Menenti, 2014). The clear relationship reported between PMI and the rate of spread has a direct physical interpretation, as LFMC controls flame propagation (Rothermel, 1972, 1991; Andrews et al., 2013; Finney, 1998; Wilson, 1990). The fact that LST anomaly is not as good as a covariate of the rate of spread suggests that the initial hypothesis of interpreting it as a measure of vegetation water stress, and indirectly of moisture content, is not able to explain the results reported in this study.

LST anomaly is a measure of the deviation of the observed LST from its climatological value. While vegetation responds to water stress through a decrease in stomatal conductance which leads to an increase of its temperature, in Mediterranean environments characterized by prolonged dry summers, this plant protection mechanism is actually triggered on a seasonal basis (Pellizzaro et al., 2007a, 2007b). This means that LST increase because of increased water stress might have already been accounted for in the LST climatology. LST anomaly may thus be unrelated to the vegetation-water stress condition and may be rather interpreted as a measure of excess enthalpy stored in fuels. This opens to a physically based interpretation of LST anomaly as a covariate of fire duration, a fire characteristic substantially unrelated to PMI. Several environmental and anthropic factors have been found to affect fire duration (Gustafson et al., 2011; Fischer et al., 2015; Costafreda-Aumedes et al., 2016; Lasslop and Kloster, 2017), but from a fire behaviour point of view, duration is rather a measure of the probability of extinction, which is the resultant of heat fluxes between the flaming zone, the surrounding fuels, and the atmosphere (Finney et al., 2013). Higher heat content in the fuels imply that less endothermic enthalpy is needed to sustain fire spread, this resulting in a lower

probability of extinction (Wilson, 1985, 1990; Albini, 1985, 1986). The interpretation of LST anomaly as a measure of excess enthalpy thus justifies its effect on fire duration.

The weak decreasing trend observed between LST anomaly and rate of spread may be susceptible of a similar physical interpretation. Heat fluxes between burning material and the surrounding fuels are at the basis of flame propagation, and rate of spread is determined by the ratio between the heat flux received by the fuels from the heat source and the heat required to achieve ignition (Rothermel, 1972; Weber, 1991). While the latter is dependent on fuel moisture content, the former is determined by convective and radiative heat exchange (Albini, 1985; Baines, 1990). Convective heat exchange is dependent on temperature difference and on a heat exchange coefficient weakly dependent on the same temperature difference. A higher fuel temperature might thus lead to slower flame propagation. Clearly, LST anomaly values observed in this study cannot be considered as a driver of the rate of spread as LFMC (as measured by PMI). However, this interpretation may explain the observed weakly decreasing trends in rate of spread with increasing LST anomaly.

4.5 Joint use of LST anomaly and PMI for the prediction of extreme events

It was discussed that LST anomaly and PMI are good predictors of fire duration and rate of spread respectively, and this was justified through the outlined physical interpretation. Their independence was also noted. As these two remote sensing observations of fuel condition are both strong predictors of burned area, this opened an opportunity for their joint use for the evaluation of the probability of extreme events. Indeed, if burned area is considered as a resultant, among the other factors, of rate of spread and fire duration, it is reasonable to expect that the joint use of LST anomaly and PMI may lead to better predictions. The adopted approach was to model the parameters of the probability distribution of log-transformed burned area as a function of these two remote sensing observables. Findings discussed herein reasonably allowed the use of linear models. From these, the probability of extreme events, conditional to ignition could be evaluated as a function of LST anomaly and PMI. Extreme events were here defined as those exceeding the 95th percentile of all burned area values recorded in the study area, which is 30 ha. The probability of fires larger than 30.0 ha conditional to ignition shows a ten-fold increase from 0.9% to 9.2% when LST anomaly increases from −2.1 to 4.3 K, and a four-fold increase from 1.8% to 7.4% when PMI decreases from 0.052 to −0.032 (Fig. 10.10). Extending this line of reasoning, bivariate linear models were constructed for the mean and the standard deviation

of the normal distribution of log-transformed burned area, leading to a model predicting the probability of extreme events, conditional to ignition, as a function of both LST anomaly and PMI. The joint model, when evaluated over the same range of LST anomaly and PMI values (−2.1 to 4.3 K and 0.052 to −0.032, respectively), shows that the probability of fires larger than 30.0 ha conditional to ignition varies between 0.5% and 12.7% (Fig. 10.11), that is, a 25-fold increase. The wider dynamic range attained confirms the stated hypothesis that the joint use of LST anomaly and PMI can lead to improved predictions.

5 Conclusions

Fire danger is defined as 'the resultant, often expressed as an index, of both constant and variable factors affecting the inception, spread, and difficulty of control of fires and the damage they cause' (FAO, 1986). The concept of danger is semantically related to a human perception (Bachmann and Allgöwer, 2000). FAO definition, through the reference to difficulty of control, acknowledges fire behaviour and its resultants (such as burned area and fire duration) as components of fire danger (Allgöwer et al., 2003). Fire danger indices available to decision makers and fire managers reflect this and mainly focus on the prediction of fire occurrence—the inception and spread in FAO's definition—and behaviour. This study sits on the fire behaviour side of fire danger, with this being a novelty as a remote sensing application, and contributes to the identified need to improve fire danger models (Ruffault et al., 2018; Schunk et al., 2017; Jolly, 2007; Jolly and Johnson, 2018; Nolan et al., 2018; Pellizzaro et al., 2007b; Rossa and Fernandes, 2017; Rossa et al., 2016), through an understanding of how prefire satellite observations of live fuel conditions are related to fire characteristics such as burned area, fire duration, and rate of spread.

Crucial to the proposed probabilistic approach was the identification of the best-fitting probability models describing burned area, fire duration, and rate of spread. The probability distribution of fire characteristics is shaped by the unique combination of topography, land use/land cover, land management practices, and human settlements characterizing each region, and the adoption of models fitting data in other areas worldwide is not appropriate (Reed and McKelvey, 2002; Cui and Perera, 2008). Once the distributions of burned area, fire duration, and rate of spread have been modelled, the study focussed on the evaluation of the corresponding probability models conditional to LST anomaly, PMI, and FWI components.

It was shown that LST anomaly is a strong covariate of fire duration and a weak covariate of rate of spread, whereas PMI is a strong covariate

of rate of spread. Both remote sensing quantities are strong predictors of burned area. These results raise an important opportunity to map probability of extreme events, conditional to ignition, with prefire estimations of LST anomaly and PMI. In this study, an event is considered extreme if burned area, duration, or rate of spread exceeds the 95th percentile of historical values in the region. Once the dependence of the parameters of the probability distribution of a fire characteristic is modelled against LST anomaly (respectively, PMI), the probability of extreme events, conditional to ignition, is a function of LST anomaly (respectively, PMI). As expected, it was found that an increasing LST anomaly and a decreasing PMI (decreasing LFMC) lead to increased probability of extreme events.

This study also investigated complementarity of remote sensing measurements of live fuel condition with the well-consolidated FWI system, especially in terms of the prediction of rate of spread. The approach for this evaluation followed the same line of reasoning adopted for remote sensing observations of live fuel status, i.e., the parameters of the probability distribution functions of burned area, fire duration, and rate of spread conditional to FWI system components were analysed to identify trends. It was found that all FWI system components control burned area, albeit to a different extent, and that similar results apply to fire duration. It was also found that the parameters of the probability distribution of the rate of spread are insensitive to FWI system components. Relative performance of the probability distribution models conditional to LST anomaly, PMI, and the six FWI system components was assessed, and it was shown that models conditional to remote sensing observations are characterized by a higher likelihood. This result is not final, considering the stated complementarity of the remote sensing and meteorological approaches with fuel condition being observed by the former and modelled by the latter. However, it must be remarked how, in the study area, remote sensing in the optical domain was a predictor of rate of spread, whereas FWI system components were not.

While LST anomaly and PMI can be used individually to predict the fire characteristics that they control, this study tested the advantage of their synergistic use in the prediction of burned area. This approach was supported by the demonstrated independence of LST anomaly and PMI. The probability of large fires conditional to ignition as a function of both LST anomaly and PMI covers a broader range of values as compared to the same probability evaluated as a function of these two remote sensing quantities individually. The outlined approach is clearly open to further integration with traditional fire danger indices such as the FWI, but this was outside the scope of this study.

To the best of the authors' knowledge, this study delivered a few novelties both in the metrics being developed for the assessment of live fuel condition and in the approach aiming at quantifying probabilities of

extreme events, conditional to ignition, as a function of remote sensing measurements. By focussing on fire behaviour characteristics, it further opened new opportunities to use remote sensing for fire danger mapping, whereas its potential for the prediction of fire occurrence has already been demonstrated by several scholars.

The probabilistic approach proposed in this study is closer to the fire management needs, where the main concern is about the odds of facing complex operational scenarios associated with extreme events (Gunes and Kovel, 2000; North et al., 2015; Oliveira et al., 2017; Thompson et al., 2015). The fact that all results reported herein refer to prefire remote sensing observations of live fuel condition may allow the production of predictive maps. The complementarity of remote sensing and traditional meteorological fire danger indices concerning both fuel condition and fire behaviour characteristics carries added value to fire managers.

This research was performed in a relatively wide and diverse region in the middle of the Mediterranean. However, extrapolation to other areas worldwide is not immediate for two main reasons. The first refers to the need to identify the probability model fitting burned area, fire duration, and rate of spread. It was already discussed how transferring models from other areas would not be correct. Further, local environmental conditions and vegetation communities shape fuel composition and may alter the relationship between fire behaviour and remote sensing of fuel condition. It can be expected that separate regional predictive models may be created within the same methodological framework at the basis of this study. This is feasible as fire inventories in some of the most fire prone areas worldwide are either publicly available on the web—e.g., the Prométhée database in Mediterranean France, the Instituto da Conservação da Natureza e das Florestas (ICNF) fire inventory in Portugal, and the United States Geological Survey (USGS) fire occurrence data in the United States—or are provided upon request by relevant authorities, e.g., the Forest Fire Protection Information Unit of Carabinieri in Italy and the National Statistical Service in Greece. Nevertheless, the effectiveness of our approach would still need to be verified across different ecosystems/environment conditions and region extent.

In the future, it would be relevant to understand whether the proposed approach would work for the prediction of fire behaviour characteristics other than burned area, duration, and rate of spread. Indeed, these were indirectly derived from the data available for this research, which did not contain further information on fire behaviour. Among several fire behaviour characteristics, it would be interesting to investigate fire intensity, as this is controlled by fuel amount and condition (De Luis et al., 2004; Vilà et al., 2001) and has been found to be related to FWI system components

(Camia and Amatulli, 2009). A proxy for fire intensity is the fire radiative power (Smith and Wooster, 2005; Wooster, 2003), which is a measure of the rate of radiant heat emitted from a fire, and has the advantage of being widely available as part of the standard fire products retrieved from satellite data like MODIS, VIIRS, and SLSTR (Justice et al., 2002; Schroeder et al., 2014; Wooster et al., 2012).

A further area of development is the integration of fire danger predictions based on remote sensing measurements with existing fire danger systems based on meteorological data. The complementarity of these two approaches has already been discussed in this study. Integration of optical and thermal observations of forest condition by means of a probabilistic framework led to improved predictions of burned area. It can thus be expected that further integration with the FWI system may be beneficial. More generally, it would be relevant to study other approaches to integrate meteorological and remote sensing measurements of the fire environment, specifically model-based methodologies. The successful interpretation of the results of this study in the light of the combustion and propagation processes would encourage further research in this direction.

The discussed reproducibility of the approach introduced by this study gives way to some recommendations beyond the developments prospected above, towards operational use of satellite remote sensing in fire danger mapping. The first and more relevant is to ensure that models linking remote sensing of forest condition to the probability of extreme events are adapted to the operational scenarios where they would be used. In addition to the discussed adaptation to the regional landscape characteristics, it would be specifically important to define with fire managers what is the magnitude of an extreme event, from their point of view. In this study a conventional threshold was used, corresponding to the 95th percentile of the historical values of fire behaviour characteristic of interest (e.g., burned area), but fire managers might want to advise otherwise.

Indeed, it is essential to work closely with end users to ensure data potential and limitations are properly understood. This study measured danger as the probability, conditional to ignition, of a fire characteristic of interest exceeding a threshold value. Other mechanisms of representation could be considered, such as a multiplier against a baseline probability, thus giving an immediate measure of increasing danger during the dry season. In fact, any remote sensing fire danger monitoring service should be meant to support an informed and sound decision-making process, and attention should be paid to the point of view of the user on data usage and interpretation, which might not necessarily coincide with that of the scientist or of the service provider.

Acknowledgements

This case study is widely based on material created by the authors and published under the CC-BY and the CC-BY-SA licences.

We acknowledge the support of the *Carabinieri* (Italian national gendarmerie) Forest Fire Protection Information Unit (*Nucleo Informativo Antincendio Boschivo*). They provided, in collaboration with *Dipartimento della Protezione Civile* (Italian Civil Protection Department), the fire data used in this study.

This study was entirely based on the use of open-source software: GDAL/OGR (GDAL/OGR Contributors, 2021), GNU Octave (Eaton et al., 2020) with HANTS (Abouali, 2021), GRASS GIS (GRASS Development Team, 2020), Python (van Rossum and de Boer, 1991), QGIS (QGIS Development Team, 2021), and R (R Core Team, 2020) with packages caret (Kuhn, 2021), evd (Stephenson, 2002), fitdistrplus (Delignette-Muller and Dutang, 2015), ggplot2 (Wickham, 2016), trend (Pohlert, 2020). The silent work of their respective communities is a powerful enabler of research and innovation.

References

Abbott, K.N., Leblon, B., Staples, G.C., Maclean, D.A., Alexander, M.E., 2007. Fire danger monitoring using RADARSAT-1 over northern boreal forests. Int. J. Remote Sens. 28 (6), 1317–1338. Available from: https://www.tandfonline.com/doi/full/10.1080/01431160600904956. doi:10.1080/01431160600904956.

Abdollahi, M., Islam, T., Gupta, A., Hassan, Q.K., 2018. An advanced forest fire danger forecasting system: integration of remote sensing and historical sources of ignition data. Remote Sens. 10 (6), 923. Available from: http://www.mdpi.com/2072-4292/10/6/923. doi:10.3390/rs10060923.

Abouali, M., 2021. MATLAB Central File Exchange MATLAB Implementation of Harmonic ANalysis of Time Series (HANTS). https://www.mathworks.com/matlabcentral/fileexchange/38841-matlab-implementation-of-harmonic-analysis-of-time-series-hants

Albini, F.A., 1985. A model for fire spread in wildland fuels by radiation. Combust. Sci. Technol. 42 (5-6), 229–258. Available from: http://www.tandfonline.com/doi/abs/10.1080/00102208508960381. doi:10.1080/00102208508960381.

Albini, F.A., 1986. Wildland fire spread by radiation – a model including fuel cooling by natural convection. Combust. Sci. Technol. 45 (1-2), 101–113. Available from: https://www.tandfonline.com/doi/full/10.1080/00102208608923844. doi:10.1080/00102208608923844.

Alfieri, S.M., De Lorenzi, F., Menenti, M., 2013. Mapping air temperature using time series analysis of LST: the SINTESI approach. Nonlinear Process. Geophys. 1023-5809. 20 (4), 513–527. Available from: http://www.nonlin-processes-geophys.net/20/513/2013/. doi:10.5194/npg-20-513-2013.

Allgöwer, B., Carlson, J.D., van Wagtendonk, J.W., 2003. Introduction to fire danger rating and remote sensing – will remote sensing enhance wildland fire danger rating? Wildland Fire Danger Estimation and Mapping – the Role of Remote Sensing Data. World Sci., 1–19. Available from: http://www.worldscientific.com/doi/abs/10.1142/9789812791177_0001. doi:10.1142/9789812791177_0001.

Amato, V., Valletta, M., 2017. Wine landscapes of Italy. In: Landscapes and Landforms of Italy. Springer International Publishing, Cham, pp. 523–536. Available from: http://link.springer.com/10.1007/978-3-319-26194-2. doi:10.1007/978-3-319-26194-2.

Anderson, T.W., Darling, D.A., 1954. A test of goodness of fit. J. Am. Stat. Assoc. 0162-1459. 49 (268), 765–769. Available from: http://www.tandfonline.com/doi/abs/10.1080/01621459.1954.10501232. doi:10.1080/01621459.1954.10501232.

Andrews, P.L., 2007. BehavePlus fire modeling system: past, present, and future. In: 2007 Proceedings of 7th Symposium on Fire and Forest Meteorology. American Meteorological Society, Bar Harbor, p. 13.

Andrews, P.L., Cruz, M.G., Rothermel, R.C., 2013. Examination of the wind speed limit function in the Rothermel surface fire spread model. Int. J. Wildland Fire 22 (7), 959–969. Available from: http://www.publish.csiro.au/?paper=WF12122. doi:10.1071/WF12122.

Bachmann, A., Allgöwer, B., 2000. The need for a consistent wildfire risk terminology. In: Crossing the Millennium: Integrating Spatial Technologies and Ecological Principles for a New Age in Fire Management, p. 67–77.

Baines, P.G., 1990. Physical mechanisms for the propagation of surface fires. Math. Comput. Model. 08957177. 13 (12), 83–94. Available from: https://linkinghub.elsevier.com/retrieve/pii/089571779090102S. doi:10.1016/0895-7177(90)90102-S.

Baker, W.L., 1989. Landscape ecology and nature reserve design in the Boundary Waters Canoe Area, Minnesota. Ecology 70 (1), 23–35. Available from: http://doi.wiley.com/10.2307/1938409. doi:10.2307/1938409.

Bond, W.J., Woodward, F.I., Midgley, G.F., 2005. The global distribution of ecosystems in a world without fire. New Phytol. 1469-8137. 165 (2), 525–538. Available from: http://doi.wiley.com/10.1111/j.1469-8137.2004.01252.x. doi:10.1111/j.1469-8137.2004.01252.x.

Bowd, E.J., Banks, S.C., Strong, C.L., Lindenmayer, D.B., 2019. Long-term impacts of wildfire and logging on forest soils. Nat. Geosci. 12 (2), 113–118. Available from: http://www.nature.com/articles/s41561-018-0294-2. doi:10.1038/s41561-018-0294-2.

Buitrago Acevedo, M.F., Groen, T.A., Hecker, C.A., Skidmore, A.K., 2017. Identifying leaf traits that signal stress in TIR spectra. ISPRS J. Photogramm. Remote Sens. 125, 132–145. Available from: https://linkinghub.elsevier.com/retrieve/pii/S0924271616301927. doi:10.1016/j.isprsjprs.2017.01.014.

Burgan, R.E., 1988. Revisions to the 1978 National Fire-Danger Rating System. U.S. Department of Agriculture, Forest Service, Southeastern Forest Experiment Station Asheville.

Camia, A., Amatulli, G., 2009. Weather factors and fire danger in the Mediterranean. In: Earth Observation of Wildland Fires in Mediterranean Ecosystems. Springer Berlin Heidelberg, Berlin, pp. 71–82. Available from: http://link.springer.com/10.1007/978-3-642-01754-4_6. doi:10.1007/978-3-642-01754-4_6.

Carlson, J.D., Burgan, R.E., 2003. Review of users' needs in operational fire danger estimation: the Oklahoma example. Int. J. Remote Sens. 24 (8), 1601–1620. Available from: https://www.tandfonline.com/doi/full/10.1080/01431160210144651. doi:10.1080/01431160210144651.

Ceccato, P., Flasse, S., Grégoire, J.-M., 2002. Designing a spectral index to estimate vegetation water content from remote sensing data: part 2. Validation and applications. Remote Sens. Environ. 0034-4257. 82, 198–207. doi:10.1016/S0034-4257(02)00036-6.

Certini, G., 2005. Effects of fire on properties of forest soils: a review. Oecologia 0029-8549. 143 (1), 1–10. Available from: http://link.springer.com/10.1007/s00442-004-1788-8. doi:10.1007/s00442-004-1788-8.

Chowdhury, E.H., Hassan, Q.K., 2015a. Development of a new daily-scale Forest Fire Danger Forecasting System using remote sensing data. Remote Sens. 2072-4292. 7 (3), 2431–2448. Available from: http://www.mdpi.com/2072-4292/7/3/2431. doi:10.3390/rs70302431.

Chowdhury, E.H., Hassan, Q.K., 2015b. Operational perspective of remote sensing-based forest fire danger forecasting systems. ISPRS J. Photogramm. Remote Sens. 0924-2716. 104, 224–236. Available from: https://linkinghub.elsevier.com/retrieve/pii/S0924271614000835. doi:10.1016/j.isprsjprs.2014.03.011.

Chuvieco, E., Wagtendonk, J., Riaño, D., Yebra, M., Ustin, S.L., 2009. Estimation of fuel conditions for fire danger assessment. In: Earth Observation of Wildland Fires in Mediterranean Ecosystems. Springer Berlin Heidelberg, Berlin, pp. 83–96. Available from: http://link.springer.com/10.1007/978-3-642-01754-4_7. doi:10.1007/978-3-642-01754-4_7.

Corral, Á., Telesca, L., Lasaponara, R., 2008. Scaling and correlations in the dynamics of forest-fire occurrence. Phys. Rev. E 77, 016101. Available from: https://link.aps.org/doi/10.1103/PhysRevE.77.016101. doi:10.1103/PhysRevE.77.016101.

Costafreda-Aumedes, S., Cardil, A., Molina, D.M., Daniel, S.N., Mavsar, R., Vega-Garcia, C., 2016. Analysis of factors influencing deployment of fire suppression resources in Spain using artificial neural networks. iForest Biogeosci. Forestry 9 (1), 138–145. Available from: http://www.sisef.it/iforest/?doi=ifor1329-008. doi:10.3832/ifor1329-008.

Cui, W., Perera, A.H., 2008. What do we know about forest fire size distribution, and why is this knowledge useful for forest management? Int. J. Wildland Fire 17 (2), 234–244. Available from: http://www.publish.csiro.au/?paper=WF06145. doi:10.1071/WF06145.

Cumming, S.G., 2001. A parametric model of the fire-size distribution. Can. J. For. Res. 0045-5067. 31, 1297–1303. doi:10.1139/x01-032.

Dasgupta, S., Qu, J.J., Hao, X., 2006. Design of a susceptibility index for fire risk monitoring. IEEE Geosci. Remote Sens. Lett. 3 (1), 140–144. Available from: http://ieeexplore.ieee.org/document/1576707/. doi:10.1109/LGRS.2005.858484.

Dasgupta, S., Qu, J.J., Hao, X., Bhoi, S., 2007. Evaluating remotely sensed live fuel moisture estimations for fire behavior predictions in Georgia, USA. Remote Sens. Environ. 0034-4257. 108 (2), 138–150. Available from: http://linkinghub.elsevier.com/retrieve/pii/S003442570600455X. doi:10.1016/j.rse.2006.06.023.

de Groot, W.J., Flannigan, M.D., 2014. Climate change and early warning systems for wildland fire. In: Reducing Disaster: Early Warning Systems for Climate Change. Springer Netherlands, Dordrecht, pp. 127–151. Available from: http://link.springer.com/10.1007/978-94-017-8598-3_7. doi:10.1007/978-94-017-8598-3_7.

De Luis, M., Baeza, M.J., Raventós, J., González-Hidalgo, J.C., 2004. Fuel characteristics and fire behaviour in mature Mediterranean gorse shrublands. Int. J. Wildland Fire 13 (1), 79–87. Available from: http://www.publish.csiro.au/?paper=WF03005. doi:10.1071/WF03005.

Deeming, J.E., Burgan, R.E., Cohen, J.D., 1977. The National Fire Danger Rating System – 1978. U.S. Department of Agriculture, Forest Service, Intermountain Forest and Range Experiment Station Ogden.

Delignette-Muller, M.L., Dutang, C., 2015. fitdistrplus: an R package for fitting distributions. J. Stat. Softw. 64 (4). Available from: http://www.jstatsoft.org/v64/i04/. doi:10.18637/jss.v064.i04.

Dowdy, A., James, M., Graham, A., Finkele, K., de Groot, W., 2009. Australian Fire Weather as Represented by the McArthur Forest Fire Danger Index and the Canadian Forest Fire Weather Index. Centre for Australian Weather and Climate Research Melbourne. http://citeseerx.ist.psu.edu/viewdoc/download?doi=10.1.1.307.8282&rep=rep1&type=pdf.

Ducci, D., Tranfaglia, G., 2008. Effects of climate change on groundwater resources in Campania (southern Italy). In: Geological Society. Special Publications, London, Vol. 288, 25–38. Available from: http://sp.lyellcollection.org/lookup/doi/10.1144/SP288.3. doi:10.1144/SP288.3.

Eaton, J.W., David, B., Søren, H., Rik, W., 2020. GNU Octave version 6.1.0 manual: a high-level interactive language for numerical computations. https://www.gnu.org/software/octave/doc/v6.1.0/

FAO, 1986. Wildland Fire Management Terminology. Food and Agriculture Organization of the United Nations, Rome, p. 257.

FAO, 2007. Fire Management - Global Assessment 2006. Food and Agriculture Organization of the United Nations, Rome. http://www.fao.org/docrep/009/a0969e/a0969e00.htm.

Field, R.D., Spessa, A.C., Aziz, N.A., Camia, A., Cantin, A., Carr, R., de Groot, W.J., Dowdy, A.J., Flannigan, M.D., Manomaiphiboon, K., Pappenberger, F., Tanpipat, V., Wang, X., 2015. Development of a Global Fire Weather Database. Nat. Hazards Earth Sys. Sci. 1684-9981. 15 (6), 1407–1423. Available from: https://www.nat-hazards-earth-syst-sci.net/15/1407/2015/. doi:10.5194/nhess-15-1407-2015.

Finney, M.A., 1998. FARSITE: Fire Area Simulator – Model Development and Evaluation, Ogden, p. 47. https://www.fs.usda.gov/treesearch/pubs/4617. doi:10.2737/RMRS-RP-4.

Finney, M.A., 2005. The challenge of quantitative risk analysis for wildland fire. For. Ecol. Manage. 211 (1-2), 97–108. Available from: https://linkinghub.elsevier.com/retrieve/pii/S0378112705000563. doi:10.1016/j.foreco.2005.02.010.

Finney, M.A., Cohen, J.D., McAllister, S.S., Jolly, W.M., 2013. On the need for a theory of wildland fire spread. Int. J. Wildland Fire 22 (1), 25–36. Available from: http://www.publish.csiro.au/?paper=WF11117. doi:10.1071/WF11117.

Fischer, M.A., Di Bella, C.M., Jobbágy, E.G., 2015. Influence of fuel conditions on the occurrence, propagation and duration of wildland fires: a regional approach. J. Arid Env. 120, 63–71. Available from: https://linkinghub.elsevier.com/retrieve/pii/S0140196315000944. doi:10.1016/j.jaridenv.2015.04.007.

Flannigan, M.D., Wotton, B.M., Marshall, G.A., de Groot, W.J., Johnston, J., Jurko, N., Cantin, A.S., 2016. Fuel moisture sensitivity to temperature and precipitation: climate change implications. Clim. Change 134, 59–71. Available from: http://link.springer.com/10.1007/s10584-015-1521-0. doi:10.1007/s10584-015-1521-0.

Fratianni, S., Acquaotta, F., 2017. The Climate of Italy Landscapes and Landforms of Italy. Springer International Publishing, Cham, pp. 29–38. Available from: http://link.springer.com/10.1007/978-3-319-26194-2. doi:10.1007/978-3-319-26194-2.

Gao, B.-C., 1996. NDWI – a normalized difference water index for remote sensing of vegetation liquid water from space. Remote Sens. Environ. 58 (3), 257–266. Available from: http://linkinghub.elsevier.com/retrieve/pii/S0034425796000673. doi:10.1016/S0034-4257(96)00067-3.

GDAL/OGR Contributors, 2021. Open Source Geospatial Foundation GDAL/OGR Geospatial Data Abstraction software Library. https://gdal.org

GRASS Development Team, 2020. Open Source Geospatial Foundation Geographic Resources Analysis Support System (GRASS) Software. https://grass.osgeo.org

Griffiths, D., 1999. Improved formula for the drought factor in McArthur's forest fire danger meter. Aust. For. 62 (2), 202–206. Available from: http://www.tandfonline.com/doi/abs/10.1080/00049158.1999.10674783. doi:10.1080/00049158.1999.10674783.

Gudmundsson, L., Rego, F.C., Rocha, M., Seneviratne, S.I., 2014. Predicting above normal wildfire activity in southern Europe as a function of meteorological drought. Environ. Res. Lett. 9 (8), 084008. Available from: http://stacks.iop.org/1748-9326/9/i=8/a=084008?key=crossref.87d2200e642c655afbcebea7fff87774. doi:10.1088/1748-9326/9/8/084008.

Gunes, A.E., Kovel, J.P., 2000. Using GIS in emergency management operations. J. Urban Plan. Dev. 126 (3), 136–149. Available from: http://ascelibrary.org/doi/10.1061/%28ASCE%290733-9488%282000%29126%3A3%28136%29. doi:10.1061/(ASCE)0733-9488(2000)126:3(136).

Gustafson, E.J., Shvidenko, A.Z., Scheller, R.M., 2011. Effectiveness of forest management strategies to mitigate effects of global change in south-central Siberia. Can. J. For. Res. 0045-5067. 41 (7), 1405–1421. Available from: http://www.nrcresearchpress.com/doi/10.1139/x11-065. doi:10.1139/x11-065.

Harvey, B.J., Donato, D.C., Turner, M.G., 2016. High and dry: post-fire tree seedling establishment in subalpine forests decreases with post-fire drought and large stand-replacing burn patches. Available from:. Glob Ecol. Biogeogr. 1466-8238. 25 (6), 655–669. doi:10.1111/geb.12443.

Haydon, D.T., Friar, J.K., Pianka, E.R., 2000. Fire-driven dynamic mosaics in the Great Victoria Desert, Australia. Landsc. Ecol. 15 (4), 373–381. Available from: http://link.springer.com/10.1023/A:1008138029197. doi:10.1023/A:1008138029197.

Hernandez, C., Keribin, C., Drobinski, P., Turquety, S., 2015. Statistical modelling of wildfire size and intensity: a step toward meteorological forecasting of summer extreme fire risk.

Ann. Geophys. 1495-2015. 33 (12), 1495–1506. Available from: http://www.ann-geophys.net/33/1495/2015/. doi:10.5194/angeo-33-1495-2015.

Hsiao, T.C., 1973. Plant responses to water stress. Annu. Rev. Plant Physiol. 24, 519–570. Available from: http://www.annualreviews.org/doi/10.1146/annurev.pp.24.060173.002511. doi:10.1146/annurev.pp.24.060173.002511.

Huesca, M., Litago, J., Merino-de-Miguel, S., Cicuendez-López-Ocaña, V., Palacios-Orueta, A., 2014. Modeling and forecasting MODIS-based Fire Potential Index on a pixel basis using time series models. Int. J. Appl. Earth Observ. Geoinf. 26, 363–376. Available from: https://linkinghub.elsevier.com/retrieve/pii/S0303243413001025. doi:10.1016/j.jag.2013.09.003.

Huesca, M., Litago, J., Palacios-Orueta, A., Montes, F., Sebastián-López, A., Escribano, P., 2009. Assessment of forest fire seasonality using MODIS fire potential: a time series approach. Agric. For. Meteorol. 0168-1923. 149 (11), 1946–1955. Available from: http://linkinghub.elsevier.com/retrieve/pii/S0168192309001658. doi:10.1016/j.agrformet.2009.06.022.

Hunt, E.R., Li, L., Tugrul Yilmaz, M., Jackson, T.J., 2011. Comparison of vegetation water contents derived from shortwave-infrared and passive-microwave sensors over central Iowa. Remote Sens. Environ. 115 (9), 2376–2383. Available from: https://linkinghub.elsevier.com/retrieve/pii/S0034425711001659. doi:10.1016/j.rse.2011.04.037.

Hunt, E.R., Ustin, S.L., Riaño, D., 2013. Remote sensing of leaf, canopy, and vegetation water contents for satellite environmental data records. In: Satellite-based Applications on Climate Change. Springer, Dordrecht, pp. 335–357. Available from: http://link.springer.com/10.1007/978-94-007-5872-8_20. doi:10.1007/978-94-007-5872-8_20.

Jackson, R.D., Idso, S.B., Reginato, R.J., Pinter, P.J., 1981.Canopy temperature as a crop water stress indicator. Water Resour. Res. 0043-1397. 17 (4), 1133–1138. doi:10.1029/WR017i004p01133.

Jolly, W.M., 2007. Sensitivity of a surface fire spread model and associated fire behaviour fuel models to changes in live fuel moisture. Int. J. Wildland Fire 16 (4), 503–509. Available from: http://www.publish.csiro.au/?paper=WF06077. doi:10.1071/WF06077.

Jolly, W.M., Johnson, D.M., 2018. Pyro-ecophysiology: shifting the paradigm of live wildland fuel research. Fire 1 (1), 8. Available from: http://www.mdpi.com/2571-6255/1/1/8. doi:10.3390/fire1010008.

Justice, C.O., Giglio, L., Korontzi, S., Owens, J., Morisette, J.T., Roy, D., Descloitres, J., Alleaume, S., Petitcolin, F., Kaufman, Y.J., 2002. The MODIS fire products. Remote Sens. Environ. 83 (1-2), 244–262. Available from: http://linkinghub.elsevier.com/retrieve/pii/S0034425702000767. doi:10.1016/S0034-4257(02)00076-7.

Kalma, J.D., McVicar, T.R., McCabe, M.F., 2008. Estimating land surface evaporation: a review of methods using remotely sensed surface temperature data. Surv. Geophys. 0169-3298. 29, 421–469. Available from: http://link.springer.com/10.1007/s10712-008-9037-z. doi:10.1007/s10712-008-9037-z.

Karnieli, A., Agam, N., Pinker, R.T., Anderson, M., Imhoff, M.L., Gutman, G.G., Panov, N., Goldberg, A., 2010. Use of NDVI and land surface temperature for drought assessment: merits and limitations. J. Clim. 1520-0442. 23 (3), 618–633. Available from: http://journals.ametsoc.org/doi/abs/10.1175/2009JCLI2900.1. doi:10.1175/2009JCLI2900.1.

Keetch, J.J., Byram, G.M., 1968. A Drought Index for Forest Fire Control. U.S.D.A. Forest Service Reseaech Paper SE-38 35 35. U.S. Department of Agriculture, Forest Service, Southeastern Forest Experiment Station, Asheville, NC.

Kendall, M.G., 1975. Rank Correlation Methods, 4th ed. Oxford University Press, New York, p. 202.

Krebs, P., Pezzatti, G.B., Mazzoleni, S., Talbot, L.M., Conedera, M., 2010. Fire regime: history and definition of a key concept in disturbance ecology. Theory Biosci. 129 (1), 53–69. Available from: http://link.springer.com/10.1007/s12064-010-0082-z. doi:10.1007/s12064-010-0082-z.

Kuhn, M., 2021. caret: Classification and Regression Training. https://cran.r-project.org/package=caret

Lasslop, G., Coppola, A.I., Voulgarakis, A., Yue, C., Veraverbeke, S., 2019. Influence of fire on the carbon cycle and climate. Curr. Clim. Change Rep. 5 (2), 112–123. Available from: http://link.springer.com/10.1007/s40641-019-00128-9. doi:10.1007/s40641-019-00128-9.

Lasslop, G., Kloster, S., 2017. Human impact on wildfires varies between regions and with vegetation productivity. Environ. Res. Lett. 12 (11), 115011. Available from: http://stacks.iop.org/1748-9326/12/i=11/a=115011?key=crossref.ebd4f5a84c83e37c43b6550c9fe5c5d0. doi:10.1088/1748-9326/aa8c82.

Leblon, B., 2005. Monitoring forest fire danger with remote sensing. Nat. Hazards 35 (3), 343–359. Available from: http://link.springer.com/10.1007/s11069-004-1796-3. doi:10.1007/s11069-004-1796-3.

Leblon, B., Kasischke, E., Alexander, M.E., Doyle, M., Abbott, M., 2002. Fire danger monitoring using ERS-1 SAR images in the case of northern boreal forests. Nat. Hazards 27 (3), 231–255. doi:10.1023/A:1020375721520.

Leblon, B., San-Miguel-Ayanz, J., Bourgeau-Chavez, L., Kong, M., 2016. Remote Sensing of Wildfires Land Surface Remote Sensing. Elsevier, London, 55–95. Available from: https://linkinghub.elsevier.com/retrieve/pii/B9781785481055500037. doi:10.1016/B978-1-78548-105-5.50003-7.

Lehsten, V., Tansey, K., Balzter, H., Thonicke, K., Spessa, A., Weber, U., Smith, B., Arneth, A., 2009. Estimating carbon emissions from African wildfires. Biogeosciences 6 (3), 349–360. doi:10.5194/bg-6-349-2009.

Lindner, M., Maroschek, M., Netherer, S., Kremer, A., Barbati, A., Garcia-Gonzalo, J., Seidl, R., Delzon, S., Corona, P., Kolström, M., Lexer, M.J., Marchetti, M., 2010. Climate change impacts, adaptive capacity, and vulnerability of European forest ecosystems. For. Ecol. Manage. 0378-1127. 259 (4), 698–709. Available from: http://linkinghub.elsevier.com/retrieve/pii/S0378112709006604. doi:10.1016/j.foreco.2009.09.023.

Littell, J.S., Peterson, D.L., Riley, K.L., Liu, Y., Luce, C.H., 2016. A review of the relationships between drought and forest fire in the United States. Glob. Change Biol. 1365-2486. 22 (7), 2353–2369. Available from: http://doi.wiley.com/10.1111/gcb.13275. doi:10.1111/gcb.13275.

Liu, Y., Wu, C., Peng, D., Xu, S., Gonsamo, A., Jassal, R.S., Altaf Arain, M., Lu, L., Fang, B., Chen, J.M., 2016. Improved modeling of land surface phenology using MODIS land surface reflectance and temperature at evergreen needleleaf forests of central North America. Remote Sens. Environ. 0034-4257. 176, 152–162. Available from: http://linkinghub.elsevier.com/retrieve/pii/S0034425716300219. doi:10.1016/j.rse.2016.01.021.

Ma, S., Zhou, Y., Gowda, P.H., Dong, J., Zhang, G., Kakani, V.G., Wagle, P., Chen, L., Colton Flynn, K., Jiang, W., 2019. Application of the water-related spectral reflectance indices: a review. Ecol. Indic. 98, 68–79. Available from: https://linkinghub.elsevier.com/retrieve/pii/S1470160X18308215. doi:10.1016/j.ecolind.2018.10.049.

Maffei, C., Alfieri, S.M., Menenti, M., 2018. Relating spatiotemporal patterns of forest fires burned area and duration to diurnal land surface temperature anomalies. Remote Sens. 10 (11), 1777. Available from: http://www.mdpi.com/2072-4292/10/11/1777. doi:10.3390/rs10111777.

Maffei, C., Lindenbergh, R., Menenti, M., 2021. Combining multi-spectral and thermal remote sensing to predict forest fire characteristics. ISPRS J. Photogramm. Remote Sens. 0924-2716. 181, 400–412. doi:10.1016/j.isprsjprs.2021.09.016.

Maffei, C., Menenti, M., 2014. A MODIS-based perpendicular moisture index to retrieve leaf moisture content of forest canopies. Int. J. Remote Sens. 35 (5), 1829–1845. Available from: http://www.tandfonline.com/doi/abs/10.1080/01431161.2013.879348. doi:10.1080/01431161.2013.879348.

Maffei, C., Menenti, M., 2019. Predicting forest fires burned area and rate of spread from pre-fire multispectral satellite measurements. ISPRS J. Photogramm. Remote Sens. 158, 263–278. Avail-

able from: https://linkinghub.elsevier.com/retrieve/pii/S0924271619302515. doi:10.1016/j.isprsjprs.2019.10.013.

Mann, H.B., 1945. Nonparametric tests against trend. Econometrica 13 (3), 245–259. doi:10.2307/1907187.

Manzo-Delgado, L., Aguirre-Gómez, R., Álvarez, R., 2004. Multitemporal analysis of land surface temperature using NOAA-AVHRR: preliminary relationships between climatic anomalies and forest fires. Int. J. Remote Sens. 25 (20), 4417–4424. Available from: http://www.tandfonline.com/doi/abs/10.1080/01431160412331269643. doi:10.1080/01431160412331269643.

Martell, D.L., 2007. Forest fire management. In: Handbook of Operations Research in Natural Resources. Springer US, Boston, MA, pp. 489–509. Available from: http://link.springer.com/10.1007/978-0-387-71815-6_26. doi:10.1007/978-0-387-71815-6_26.

Maselli, F., Romanelli, S., Bottai, L., Zipoli, G., 2003. Use of NOAA-AVHRR NDVI images for the estimation of dynamic fire risk in Mediterranean areas. Remote Sens. Environ. 86 (2), 187–197. Available from: https://linkinghub.elsevier.com/retrieve/pii/S0034425703000993. doi:10.1016/S0034-4257(03)00099-3.

Masuoka, E., Fleig, A., Wolfe, R.E., Patt, F., 1998. Key characteristics of MODIS data products. IEEE Trans. Geosci. Remote Sens. 36 (4), 1313–1323. Available from: http://ieeexplore.ieee.org/document/701081/. doi:10.1109/36.701081.

Matin, M.A., Chitale, V.S., Murthy, M.S.R., Uddin, K., Bajracharya, B., Pradhan, S., 2017. Understanding forest fire patterns and risk in Nepal using remote sensing, geographic information system and historical fire data. Int. J. Wildland Fire 1448-5516. 26 (4), 276–286. Available from: http://www.publish.csiro.au/?paper=WF16056. doi:10.1071/WF16056.

Mazzetti, P., Nativi, S., Angelini, V., Verlato, M., Fiorucci, P., 2009. A grid platform for the European Civil Protection e-Infrastructure: the forest fires use scenario. Earth Sci. Inf. 2, 53–62. Available from: http://link.springer.com/10.1007/s12145-009-0025-8. doi:10.1007/s12145-009-0025-8.

McArthur, A.G., 1967. Fire Behaviour in Eucalypt Forests. Australia Forestry and Timber Bureau, Canberra, pp. 36.

Menenti, M., Azzali, S., Verhoef, W., van Swol, R., 1993. Mapping agroecological zones and time lag in vegetation growth by means of Fourier analysis of time series of NDVI images. Adv. Space Res. 13 (5), 233–237. Available from: http://linkinghub.elsevier.com/retrieve/pii/027311779390550U. doi:10.1016/0273-1177(93)90550-U.

Menenti, M., Ghafarian Malamiri, H.R., Shang, H., Alfieri, S.M., Maffei, C., Jia, L., 2016. Observing the Response of Terrestrial Vegetation to Climate Variability across a Range of Time Scales by Time Series Analysis of Land Surface Temperature Multitemporal Remote Sensing. Springer International Publishing, Cham, pp. 277–315. doi:10.1007/978-3-319-47037-5_14.

Mhawej, M., Faour, G., Adjizian-Gerard, J., 2015. Wildfire likelihood's elements: a literature review. Challenges 6 (2), 282–293. Available from: http://www.mdpi.com/2078-1547/6/2/282. doi:10.3390/challe6020282.

Modugno, S., Balzter, H., Cole, B., Borrelli, P., 2016. Mapping regional patterns of large forest fires in wildland-urban interface areas in Europe. J. Environ. Manage. 172, 112–126. Available from: http://linkinghub.elsevier.com/retrieve/pii/S0301479716300548. doi:10.1016/j.jenvman.2016.02.013.

Mohamed Shaluf, I., 2008. Technological disaster stages and management. Disaster Prev. Manag. Int. J. 17 (1), 114–126. Available from: http://www.emeraldinsight.com/doi/10.1108/09653560810855928. doi:10.1108/09653560810855928.

Molod, A., Takacs, L., Suarez, M., Bacmeister, J., 2015. Development of the GEOS-5 atmospheric general circulation model: evolution from MERRA to MERRA2. Geosci. Model Dev. 1991-9603. 8 (5), 1339–1356. Available from: https://www.geosci-model-dev.net/8/1339/2015/. doi:10.5194/gmd-8-1339-2015.

Montagné-Huck, C., Brunette, M., 2018. Economic analysis of natural forest disturbances: a century of research. J. For. Econ. 32, 42–71. Available from: http://linkinghub.elsevier.com/retrieve/pii/S1104689917301150. doi:10.1016/j.jfe.2018.03.002.

Moritz, M.A., 1997. Analyzing extreme disturbance events: fire in Los Padres National Forest. Ecol. Appl. 7 (4), 1252–1262. Available from: http://www.jstor.org/stable/2641212?origin=crossref. doi:10.2307/2641212.

Nemani, R.R., Running, S.W., 1989. Estimation of regional surface resistance to evapotranspiration from NDVI and thermal-IR AVHRR data. J. Appl. Meteorol. 0894-8763. 28 (4), 276–284. Available from: http://journals.ametsoc.org/doi/abs/10.1175/1520-0450%281989%29028%3C0276%3AEORSRT%3E2.0.CO%3B2. doi:10.1175/1520-0450(1989)028<0276:EORSRT>2.0.CO;2.

Nolan, R.H., Boer, M.M., Resco de Dios, V., Caccamo, G., Bradstock, R.A., 2016. Large-scale, dynamic transformations in fuel moisture drive wildfire activity across southeastern Australia. Geophys. Res. Lett. 43 (9), 4229–4238. doi:10.1002/2016GL068614.

Nolan, R.H., Hedo, J., Arteaga, C., Sugai, T., de Dios, V.R., 2018. Physiological drought responses improve predictions of live fuel moisture dynamics in a Mediterranean forest. Agric. For. Meteorol. 263, 417–427. Available from: https://linkinghub.elsevier.com/retrieve/pii/S016819231830306X. doi:10.1016/j.agrformet.2018.09.011.

North, M.P., Stephens, S.L., Collins, B.M., Agee, J.K., Aplet, G., Franklin, J.F., Fulé, P.Z., 2015. Reform forest fire management. Science 349 (6254), 1280–1281. Available from: http://www.sciencemag.org/cgi/doi/10.1126/science.aab2356. doi:10.1126/science.aab2356.

Oliveira, S., Laneve, G., Fusilli, L., Eftychidis, G., Nunes, A., Lourenço, L., Sebastián-López, A., 2017. A common approach to foster prevention and recovery of forest fires in Mediterranean Europe. In: Mediterranean Identities - Environment, Society, Culture. IntechOpen, London, pp. 337–361. Available from: http://www.intechopen.com/books/mediterranean-identities-environment-society-cultu. doi:10.5772/intechopen.68948.

Pan, J., Wang, W., Li, J., 2016. Building probabilistic models of fire occurrence and fire risk zoning using logistic regression in Shanxi Province, China. Nat. Hazards 81 (3), 1879–1899. Available from: http://link.springer.com/10.1007/s11069-016-2160-0. doi:10.1007/s11069-016-2160-0.

Parker, R.J., Boesch, H., Wooster, M.J., Moore, D.P., Webb, A.J., Gaveau, D., Murdiyarso, D., 2016. Atmospheric CH4 and CO2 enhancements and biomass burning emission ratios derived from satellite observations of the 2015 Indonesian fire plumes. Atmos. Chem. Phys. 16 (15), 10111–10131. Available from: https://acp.copernicus.org/articles/16/10111/2016/. doi:10.5194/acp-16-10111-2016.

Pellegrini, A.F.A., Ahlström, A., Hobbie, S.E., Reich, P.B., Nieradzik, L.P., Staver, A.C., Scharenbroch, B.C., Jumpponen, A., Anderegg, W.R.L., Randerson, J.T., Jackson, R.B., 2018.Fire frequency drives decadal changes in soil carbon and nitrogen and ecosystem productivity. Nature 0008-5472. 553 (7687), 194–198. doi:10.1038/nature24668.

Pellizzaro, G., Cesaraccio, C., Duce, P., Ventura, A., Zara, P., 2007a. Relationships between seasonal patterns of live fuel moisture and meteorological drought indices for Mediterranean shrubland species. Int. J. Wildland Fire 16 (2), 232–241. Available from: http://www.publish.csiro.au/?paper=WF06081. doi:10.1071/WF06081.

Pellizzaro, G., Duce, P., Ventura, A., Zara, P., 2007b. Seasonal variations of live moisture content and ignitability in shrubs of the Mediterranean Basin. Int. J. Wildland Fire 16 (5), 633–641. Available from: http://www.publish.csiro.au/?paper=WF05088. doi:10.1071/WF05088.

Podschwit, H.R., Larkin, N.K., Steel, E.A., Cullen, A., Alvarado, E., 2018. Multi-model forecasts of very-large fire occurences during the end of the 21st century. Climate 6 (4), 100. Available from: http://www.mdpi.com/2225-1154/6/4/100. doi:10.3390/cli6040100.

Pohlert, T., 2020. trend: Non-parametric trend tests and change-point detection. https://cran.r-project.org/package=trend

Pyne, S.J., Andrews, P.L., Laven, R.D., 1996. Introduction to Wildland Fire, 2nd. John Wiley & Sons, Inc., New York, p. 767.

QGIS Development Team, 2021. QGIS Association QGIS Geographic Information System. https://www.qgis.org/

R Core Team, 2020. R Foundation for Statistical Computing Vienna, Austria R: A language and environment for statistical computing. https://www.r-project.org/

Reed, W.J., McKelvey, K.S., 2002. Power-law behaviour and parametric models for the size-distribution of forest fires. Ecol. Modell. 150 (3), 239–254. Available from: http://linkinghub.elsevier.com/retrieve/pii/S0304380001004835. doi:10.1016/S0304-3800(01)00483-5.

Reisen, F., Duran, S.M., Flannigan, M., Elliott, C., Rideout, K., 2015. Wildfire smoke and public health risk. Int. J. Wildland Fire 24 (8), 1029–1044. Available from: http://www.publish.csiro.au/?paper=WF15034. doi:10.1071/WF15034.

Roerink, G.J., Menenti, M., Verhoef, W., 2000. Reconstructing cloudfree NDVI composites using Fourier analysis of time series. Int. J. Remote Sens. 21 (9), 1911–1917. Available from: http://www.tandfonline.com/doi/abs/10.1080/014311600209814. doi:10.1080/014311600209814.

Rossa, C.G., Fernandes, P.M., 2017. On the effect of live fuel moisture content on fire-spread rate. For. Syst. 26 (3), eSC08. Available from: http://revistas.inia.es/index.php/fs/article/view/12019. doi:10.5424/fs/2017263-12019.

Rossa, C.G., Veloso, R., Fernandes, P.M., 2016. A laboratory-based quantification of the effect of live fuel moisture content on fire spread rate. Int. J. Wildland Fire 1049-8001. 25 (5), 569–573. Available from: http://www.publish.csiro.au/?paper=WF15114. doi:10.1071/WF15114.

Rothermel, R.C., 1972. A Mathematical Model to Predicting Fire Spread in Wildland Fuels. Odgen, p. 40.

Rothermel, R.C., 1991. Predicting Behavior and Size of Crown Fires in the Northern Rocky Mountains. U.S. Department of Agriculture, Forest Service, Ogden, pp. 46. https://www.fs.usda.gov/treesearch/pubs/26696. doi:10.2737/INT-RP-438.

Ruffault, J., Martin-StPaul, N., Pimont, F., Dupuy, J.-L., 2018. How well do meteorological drought indices predict live fuel moisture content (LFMC)? An assessment for wildfire research and operations in Mediterranean ecosystems. Agric. For. Meteorol. 262, 391–401. Available from: https://linkinghub.elsevier.com/retrieve/pii/S0168192318302521. doi:10.1016/j.agrformet.2018.07.031.

San-Miguel-Ayanz, J., Durrant, T., Boca, R., Libertà, G., Branco, A., de Rigo, D., Ferrari, D., Maianti, P., Artés Vivancos, T., Costa, H., Lana, F., Löffler, P., Nuijten, D., Ahlgren, A.C., Leray, T., 2018. Luxembourg Forest Fires in Europe, Middle East and North Africa 2017, p. 138. doi:10.2760/663443.

San-Miguel-Ayanz, J., Schulte, E., Schmuck, G., Camia, A., Strobl, P., Liberta, G., Giovando, C., Boca, R., Sedano, F., Kempeneers, P., McInerney, D., Withmore, C., de Oliveira, S.S., Rodrigues, M., Durrant, T., Corti, P., Oehler, F., Vilar, L., Amatulli, G., 2012. Comprehensive Monitoring of Wildfires in Europe: the European Forest Fire Information System (EFFIS). In: Approaches to Managing Disaster – Assessing Hazards, Emergencies and Disaster Impacts. InTech, Rijeka, pp. 87–108. Available from: http://www.intechopen.com/books/approaches-to-managing-disaster-assessing-hazards-emergencies-and-disaster-impacts/comprehensive-monitoring-of-wildfires-in-europe-the-european-forest-fire-information-sy. doi:10.5772/28441.

Schlobohm, P., Brain, J., 2002. Gaining an Understanding of the National Fire Danger Rating System. National Wildfire Coordinating Group, Boise.

Schroeder, W., Oliva, P., Giglio, L., Csiszar, I.A., 2014. The new VIIRS 375 m active fire detection data product: algorithm description and initial assessment. Remote Sens. Environ. 143, 85–96. doi:10.1016/j.rse.2013.12.008.

Schulze, E.-D., Lange, O.L., Kappen, L., Buschbom, U., Evenari, M., 1973. Stomatal responses to changes in temperature at increasing water stress. Planta 110 (1), 29–42. Available from: http://link.springer.com/10.1007/BF00386920. doi:10.1007/BF00386920.

Schunk, C., Wastl, C., Leuchner, M., Menzel, A., 2017. Fine fuel moisture for site- and species-specific fire danger assessment in comparison to fire danger indices. Agric. For. Meteorol. 234–235, 31–47. Available from: https://linkinghub.elsevier.com/retrieve/pii/S0168192316307262. doi:10.1016/j.agrformet.2016.12.007.

Seidl, R., Schelhaas, M.-J., Rammer, W., Verkerk, P.J., 2014.Increasing forest disturbances in Europe and their impact on carbon storage. Nat. Clim. Change 1758-6798. 4 (9), 806–810. doi:10.1038/nclimate2318.

Sen, P.K., 1968. Estimates of the regression coefficient based on Kendall's tau. J. Am. Stat. Assoc. 63 (324), 1379–1389. Available from: http://www.tandfonline.com/doi/abs/10.1080/01621459.1968.10480934. doi:10.1080/01621459.1968.10480934.

Slingsby, J.A., Moncrieff, G.R., Wilson, A.M., 2020. Near-real time forecasting and change detection for an open ecosystem with complex natural dynamics. ISPRS J. Photogramm. Remote Sens. 166, 15–25. Available from: https://linkinghub.elsevier.com/retrieve/pii/S092427162030143X. doi:10.1016/j.isprsjprs.2020.05.017.

Smith, A.M.S., Wooster, M.J., 2005. Remote classification of head and backfire types from MODIS fire radiative power and smoke plume observations. Int. J. Wildland Fire 14 (3), 249–254. Available from: http://www.publish.csiro.au/?paper=WF05012. doi:10.1071/WF05012.

Sobrino, J.A., Frate, F.D., Drusch, M., Jiménez-Muñoz, J.C., Manunta, P., Regan, A., 2016. Review of thermal infrared applications and requirements for future high-resolution sensors. IEEE Trans. Geosci. Remote Sens. 54 (5), 2963–2972. Available from: http://ieeexplore.ieee.org/document/7378483/. doi:10.1109/TGRS.2015.2509179.

Stephenson, A.G., 2002. evd: extreme value distributions. R News 2 (2). Available from: https://cran.r-project.org/doc/Rnews/.

Syphard, A.D., Sheehan, T., Rustigian-Romsos, H., Ferschweiler, K., 2018. Mapping future fire probability under climate change: does vegetation matter? PLoS ONE 13 (8), e0201680. Available from: https://dx.plos.org/10.1371/journal.pone.0201680. doi:10.1371/journal.pone.0201680.

Taylor, S.W., Alexander, M.E., 2006. Science, technology, and human factors in fire danger rating: the Canadian experience. Int. J. Wildland Fire 1049-8001. 15 (1), 121–135. Available from: http://www.publish.csiro.au/?paper=WF05021. doi:10.1071/WF05021.

Thompson, M.P., Haas, J.R., Gilbertson-Day, J.W., Scott, J.H., Langowski, P., Bowne, E., Calkin, D.E., 2015. Development and application of a geospatial wildfire exposure and risk calculation tool. Environ. Modell. Software 63, 61–72. Available from: https://linkinghub.elsevier.com/retrieve/pii/S1364815214002825. doi:10.1016/j.envsoft.2014.09.018.

Thonicke, K., Venevsky, S., Sitch, S., Cramer, W., 2008.The role of fire disturbance for global vegetation dynamics: coupling fire into a Dynamic Global Vegetation Model. Glob Ecol. Biogeogr. 0960-7447. 10 (6), 661–677. doi:10.1046/j.1466-822X.2001.00175.x.

Trenberth, K.E., Dai, A., van der Schrier, G., Jones, P.D., Barichivich, J., Briffa, K.R., Sheffield, J., 2014. Global warming and changes in drought. Nat. Clim. Change 4 (1), 17–22. Available from: http://www.nature.com/articles/nclimate2067. doi:10.1038/nclimate2067.

Ustin, S.L., Riaño, D., Koltunov, A., Roberts, D.A., Dennison, P.E., 2009. Mapping fire risk in Mediterranean ecosystems of California: vegetation type, density, invasive species, and fire frequency. In: Earth Observation of Wildland Fires in Mediterranean Ecosystems. Springer, Berlin Heidelberg, pp. 41–53. Available from: http://link.springer.com/10.1007/978-3-642-01754-4_4. doi:10.1007/978-3-642-01754-4_4.

van der Werf, G.R., Randerson, J.T., Giglio, L., Collatz, G.J., Mu, M., Kasibhatla, P.S., Morton, D.C., Defries, R.S., Jin, Y., van Leeuwen, T.T., 2010.Global fire emissions and the contribution of deforestation, savanna, forest, agricultural, and peat fires (1997-2009). Atmos. Chem. Phys. 1615-3201. 10 (23), 11707–11735. doi:10.5194/acp-10-11707-2010.

Van Nguyen, O., Kawamura, K., Trong, D.P., Gong, Z., Suwandana, E., 2015. Temporal change and its spatial variety on land surface temperature and land use changes in the Red River Delta, Vietnam, using MODIS time-series imagery. Environ. Monit. Assess.

1573-2959. 187 (7), 464. Available from: http://link.springer.com/10.1007/s10661-015-4691-3. doi:10.1007/s10661-015-4691-3.

van Rossum, G., de Boer, J., 1991. Interactively testing remote servers using the Python programming language. CWI Q. 4 (4), 283–303.

Van Wagner, C.E., 1977. Conditions for the start and spread of crown fire. Can. J. For. Res. 7 (1), 23–34. Available from: http://www.nrcresearchpress.com/doi/10.1139/x77-004. doi:10.1139/x77-004.

Van Wagner, C.E., 1987. Development and Structure of the Canadian Forest Fire Weather Index System. Canadian Forestry Service, Ottawa.

Verhoef, W., 1996. Application of Harmonic Analysis of NDVI Time Series (HANTS). In: Fourier Analysis of Temporal NDVI in the Southern African and American Continents, p. 19–24.

Vermote, E.F., El Saleous, N., Justice, C.O., Kaufman, Y.J., Privette, J.L., Remer, L., Roger, J.C., Tanré, D., 1997.Atmospheric correction of visible to middle-infrared EOS-MODIS data over land surfaces: background, operational algorithm and validation. J. Geophys. Res. Atmos. 2156-2202. 102 (D14), 17131–17141. doi:10.1029/97JD00201.

Vermote, E.F., Roger, J.-C., Ray, J.P., 2015. MODIS Surface Reflectance User's Guide – Collection 6.

Vidal, A., Pinglo, F., Durand, H., Devaux-Ros, C., Maillet, A., 1994. Evaluation of a temporal fire risk index in mediterranean forests from NOAA thermal IR. Remote Sens. Environ. 49 (3), 296–303. Available from: https://linkinghub.elsevier.com/retrieve/pii/0034425794900248. doi:10.1016/0034-4257(94)90024-8.

Viegas, D.X., 2009. Recent Forest Fire Related Accidents in Europe. Office for Official Publications of the European Communities, Luxembourg, pp. 76. doi:10.2788/50781.

Vilà, M., Lloret, F., Ogheri, E., Terradas, J., 2001. Positive fire-grass feedback in Mediterranean Basin woodlands. For. Ecol. Manage. 147 (1), 3–14. Available from: https://linkinghub.elsevier.com/retrieve/pii/S0378112700004357. doi:10.1016/S0378-1127(00)00435-7.

Walding, N.G., Williams, H.T.P., McGarvie, S., Belcher, C.M., 2018. A comparison of the US National Fire Danger Rating System (NFDRS) with recorded fire occurrence and final fire size. Int. J. Wildland Fire 27 (2), 99–113. Available from: http://www.publish.csiro.au/?paper=WF17030. doi:10.1071/WF17030.

Weber, M.G., Stocks, B.J., 1998. Forest Fires in the Boreal Forests of Canada Large Forest Fires. Backhuys Publishers, Leiden Backhuys Publishers, Leiden, pp. 215–233.

Weber, R.O., 1991. Modelling fire spread through fuel beds. Prog. Energy Combust. Sci. 17 (1), 67–82. Available from: https://linkinghub.elsevier.com/retrieve/pii/0360128591900036. doi:10.1016/0360-1285(91)90003-6.

Wickham, H., 2016. ggplot2: Elegant Graphics for Data Analysis. Springer-Verlag, New York, pp. 212.

Williams, A.P., Abatzoglou, J.T., 2016. Recent advances and remaining uncertainties in resolving past and future climate effects on global fire activity. Curr. Clim. Change Rep. 2198-6061. 2 (1), 1–14. Available from: http://link.springer.com/10.1007/s40641-016-0031-0. doi:10.1007/s40641-016-0031-0.

Wilson, R.A., 1985. Observations of extinction and marginal burning states in free burning porous fuel beds. Combust. Sci. Technol. 44, 179–193. Available from: http://www.tandfonline.com/doi/abs/10.1080/00102208508960302.doi:10.1080/00102208508960302.

Wilson, R.A., 1990. Reexamination of Rothermel's Fire Spread Equations in No-wind and No-slope Conditions. U.S. Department of Agriculture, Forest Service, Odgen.

Wooster, M.J., 2003. Fire radiative energy for quantitative study of biomass burning: derivation from the BIRD experimental satellite and comparison to MODIS fire products. Remote Sens. Environ. 86 (1), 83–107. Available from: https://linkinghub.elsevier.com/retrieve/pii/S0034425703000701. doi:10.1016/S0034-4257(03)00070-1.

Wooster, M.J., Xu, W., Nightingale, T., 2012. Sentinel-3 SLSTR active fire detection and FRP product: pre-launch algorithm development and performance evaluation using MODIS and ASTER datasets. Remote Sens. Environ. 120, 236–254. Available from: https://linkinghub.elsevier.com/retrieve/pii/S0034425712000818. doi:10.1016/j.rse.2011.09.033.

Xu, Y., Shen, Y., 2013. Reconstruction of the land surface temperature time series using harmonic analysis. Comput. Geosci. 0098-3004. 61, 126–132. Available from: http://linkinghub.elsevier.com/retrieve/pii/S0098300413002367. doi:10.1016/j.cageo.2013.08.009.

Yebra, M., Dennison, P.E., Chuvieco, E., Riaño, D., Zylstra, P., Hunt, E.R., Danson, F.M., Qi, Y., Jurdao, S., 2013. A global review of remote sensing of live fuel moisture content for fire danger assessment: moving towards operational products. Remote Sens. Environ. 0034-4257. 136, 455–468. doi:10.1016/j.rse.2013.05.029.

Zhou, J., Jia, L., Menenti, M., Gorte, B., 2016. On the performance of remote sensing time series reconstruction methods – a spatial comparison. Remote Sens. Environ. 187, 367–384. Available from: http://linkinghub.elsevier.com/retrieve/pii/S0034425716303972. doi:10.1016/j.rse.2016.10.025.

Zweifel, R., Rigling, A., Dobbertin, M., 2009.Species-specific stomatal response of trees to drought – a link to vegetation dynamics? J. Veg. Sci. 1654-1103. 20 (3), 442–454. doi:10.1111/j.1654-1103.2009.05701.x.